Influence of High-temperature Rolling and Annealing on texture evolution and mechanical properties of Mg-0.4wt%Bi alloy

M.Tech. Thesis

By

ANIK CHATTERJEE

DEPARTMENT OF METALLURGICAL ENGINEERING AND MATERIALS SCIENCE

INDIAN INSTITUTE OF TECHNOLOGY INDORE

MAY 2025

Influence of High-temperature Rolling and Annealing on texture evolution and mechanical properties of Mg-0.4wt%Bi alloy

A THESIS

Submitted in partial fulfillment of the requirements for the award of the degree

of

Master of Technology

By

ANIK CHATTERJEE

DEPARTMENT OF METALLURGICAL ENGINEERING AND MATERIALS SCIENCE

INDIAN INSTITUTE OF TECHNOLOGY INDORE

MAY 2025

INDIAN INSTITUTE OF TECHNOLOGY INDORE

CANDIDATE'S DECLARATION

I hereby certify that the work which is being presented in the thesis entitled **Influence of High-temperature Rolling and Annealing on texture evolution and mechanical properties of Mg-0.4wt%Bi alloy** in the partial fulfillment of the requirements for the award of the degree of **MASTER OF TECHNOLOGY** and submitted in the **DEPARTMENT OF METALLURGICAL ENGINEERING AND MATERIALS SCIENCE,Indian Institute Of Technology Indore**, is an authentic record of my own work carried out during the time period from August 2023 to May 2025 under the supervision of Dr. Dudekula Althaf Basha, Assistant Professor, IIT Indore.

The matter presented in this thesis has not been submitted by me for the award of any other degree of this or any other institute.

30.05.2025

Signature of the student with date
(ANIK CHATTERJEE)

This is to certify that the above statement made by the candidate is correct to the best of my/our knowledge.

30/05/2025

Signature of the Supervisor of M.Tech. thesis (with date)
(Dr. Dudekula Althaf Basha)

ANIK CHATTERJEE has successfully given his/her M.Tech. Oral Examination held on **26th May 2025**.

30/05/2025

Signature(s) of Supervisor(s) of M.Tech. thesis
(Dr. Dudekula Althaf Basha)
Date:

30/05/2025 Act.y DPGC

Convener, DPGC
Dr.Dudekula Althaf Basha
Date:

ACKNOWLEDGEMENTS

First and foremost, I would like to express my heartfelt gratitude to my research supervisor, **Dr. Dudekula Althaf Basha**, for his unwavering support, insightful guidance, and constant encouragement throughout my research journey. His approachable nature and constructive feedback have been instrumental in shaping the direction and quality of this work. Despite the demands of numerous administrative responsibilities, he always made time to engage with his students and offer thoughtful discussions on academic and research matters, for which I am sincerely grateful. I have always been inspired by his exceptional time management and his ability to articulate complex ideas in a clear and accessible manner, which greatly enhanced my conceptual understanding and enabled me to navigate my research with confidence.I also take this opportunity to extend my sincere thanks to Prof. **Sushas S. Joshi,** Director, IIT Indore**,** for providing the necessary infrastructure and institutional support that facilitated the successful completion of this research.

I sincerely thank Prof. Ajay Kumar Kushwaha, Head of MEMS, for providing the necessary facilities during my M.Tech project.I am also grateful to the department faculty for their consistent support and valuable guidance.Their efforts greatly enhanced my understanding of Metallurgical Engineering.

I am also very thankful to **Mr. Mukesh Singh and Mr. Mayank Mishra**, Research Scholar, MEMS Department for their constant encouragement, intellectual contributions, and constructive feedback that have greatly enriched my research work.

Last but not least, I cannot forget the support and encouragement received from my family and my colleagues.

DEDICATION

Dedicated to my Guide

My Parents

My Teachers

My Seniors

My Friends

Abstract

This work focuses on exploring how sequential thermomechanical processing—specifically hot rolling followed by thermal annealing—affects the microstructural features, crystallographic texture evolution, and deformation response of a Mg-0.4 wt% Bi alloy. The alloy underwent hot deformation at 300℃, after which it was subjected to annealing at three distinct temperatures: 225℃, 325℃, and 425℃. These treatments were systematically analyzed to assess their influence on grain size reduction, texture transformation, and resultant mechanical characteristics.. Scanning Electron Microscopy (SEM) revealed an increase in grain size from 19.88μm at 225℃ to 22.79μm at 325℃, indicating full recrystallization. Annealing at 425℃ resulted in a significant 61% increase in grain size, reaching 36.77μm, which reflects substantial grain growth at higher temperatures.Electron Backscatter Diffraction (EBSD) assessments performed at varying annealing temperatures revealed that as the temperature rose from 225℃ to 325℃, there was a notable decline in peak texture intensity, dropping from 22.01 to 15.10., attributed to texture weakening that leads to random nucleation of grains, However, further increase in temperature to 425℃, maximum texture intensity increased to 20.16μm, pointing to the dominating grain growth orientation. Furthermore, Kernel Average Misorientation (KAM) maps indicate a decrease in dislocation density and internal strain with increasing annealing temperature, from a KAM value of 0.55 at 325℃ to 0.11 at 425℃, confirming progressive microstructural recovery. Tensile testing showed that the as-cast and homogenized samples exhibit low strength with moderate ductility, whereas rolling at 300℃ significantly enhanced strength but reduced elongation. Optimal mechanical properties were obtained at 325℃, yielding a balanced combination of strength (YS: 91 MPa, UTS: 143 MPa) and ductility (elongation: 5.5%).The results highlight that the combination of hot rolling under controlled conditions followed by strategically selected annealing treatments can significantly influence microstructural refinement, texture adjustment, and mechanical property improvement in Mg-Bi alloys, thereby positioning them as strong contenders for use in lightweight structural components..

TABLE OF CONTENTS

LIST OF FIGURES

325°C for 10 minutes and, (c) At Φ=0°, (d) Φ=30° when rolled at 300°C and annealed at 425°C for 10 minutes.

Fig.5.9: (a) Depicts the IPF and, (b) Corresponding distribution of grain size rolled at 300°C and annealed at 225°C for 10 minutes.

Fig.5.10: (a) Depicts the IPF and, (b) Corresponding distribution of grain size rolled at 300°C and annealed at 325°C for 10 minutes.

Fig.5.11: (a) Depicts the IPF and, (b) Corresponding distribution of grain size rolled at 300°C and annealed at 425°C for 10 minutes.

Fig.5.12:Depicts the Kernel Average Misorientation (KAM) maps for Mg-0.4wt%Bi alloy, (a) Rolled at 300°C and annealed at 325°C for 10 minutes with a KAM_{avg} of 0.55 and, (b) Rolled at 300°C and annealed at 425°C for 10 minutes with a KAM_{avg} of 0.11.

Fig 5.13: Displays the SF_{avg} values for various slip systems when the Mg-0.4wt%Bi alloy is being subjected to hot rolling at 300°C followed by annealing at 225°C,325°C and 425°C for 10 minutes.

Fig 5.14: Displays the Misorientation angle distribution for alloy, (a) Rolled at 300°C and annealed at 225°C for 10 minutes, (b) Rolled at 300°C and annealed at 325°C for 10 minutes, (c) Rolled at 300°C and annealed at 425°C for 10 minutes.

Fig 5.15: Engineering stress-strain curves of Mg-0.4wt% Bi alloy in different thermo-mechanical conditions:as cast and homogenized,as-rolled at 300°C,as-rolled at 300°C and annealed at 225°C, 325°C, and 425°C for 10 minutes.

Fig 5.16:Comparison of various mechanical properties with standard deviation for different processing conditions:(i)as cast and homogenized, (ii) as-rolled at 300 °C, (iii) annealed at 225 °C for 10 min after rolling at 300 °C, (iv) annealed at 325 °C for 10 min after rolling at 300 °C, and (v) annealed at 425 °C for 10 min after rolling at 300 °C.

LIST OF TABLES

Table 5.1: Shows the Tensile properties of Mg-0.4wt% Bi alloy under different processing conditions.

NOMENCLATURE

° – Degree

%– Percentage

wt%-Weight percent

±– Plus-Minus

θ– Theta

ϕ – Phi

ρ– Density

∑– Summation

τ – Shear stress

μ– Micro

σ – Stress

ε– Strain

D_{avg} –Average diameter

SF_{avg}-Average value of Schmid Factor

LIST OF ABBREVIATIONS

Mg – Magnesium

Bi – Bismuth

REE – Rare Earth Elements

AZ91 – Aluminium zinc alloy having 9% Al and 1% Zn

RT – Room Temperature

HAZ – Heat Affected Zone

GB – Grain Boundary

SFE – Stacking Fault Energy

GBS – Grain Boundary Sliding

ADF-STEM – Annular Dark Field Scanning Transmission Electron Microscopy

DRX – Dynamic Recrystallization

TDRX – Twin-Induced Dynamic Recrystallization

TMT – Thermomechanical Treatment

HT – Heat Treatment

HCP – Hexagonal Close-Packed

CRSS – Critical Resolved Shear Stress

CTB – Coherent Twin Boundary

SE – Secondary Electron

BSE − Back Scattered Electron

PF − Pole Figure

IPF − Inverse Pole Figure

RD − Radial Direction

TD − Transverse Direction

ODF − Orientation distribution function

Chapter 1

INTRODUCTION

Magnesium-based alloys are extensively utilized in sectors such as aerospace, automotive, and biomedical engineering due to their remarkably low density and excellent specific strength. Magnesium-based alloys have found widespread application in fields such as biomedical devices, aerospace structures, and automotive components, where achieving substantial weight savings while maintaining mechanical reliability is of paramount importance. However,the broader utilization of these alloys is hindered by inherent drawbacks, including insufficient ductility, restricted formability, and resistance to corrosion. To address these issues, alloying strategies have been extensively explored, with bismuth (Bi) emerging as a promising addition due to its low toxicity, cost-effectiveness, and ability to form thermally stable intermetallic compounds like Mg_3Bi_2, which enhance mechanical performance and microstructural stability. The combination of alloy composition and thermomechanical processing plays a crucial role in optimizing Mg–Bi systems. Hot rolling, conducted above the recrystallization temperature, refines grain structures, eliminates casting defects, and activates dynamic recrystallization (DRX), & this consideration is especially critical for magnesium, as the number of active slip systems available at ambient temperature is inherently limited.. This thesis investigates the effects of hot rolling on Mg–0.4 wt% Bi alloys, focusing on the impact of high-temperature deformation followed by annealing on the development of microstructure, evolution of crystallographic texture, and the resulting mechanical behavior. Primary goal is to establish a processing–structure–property relationship that advances the metallurgical understanding of Mg– Bi systems and facilitates the development of next-generation lightweight alloys for structural applications.

1.1 Mg alloys and their properties

Among all structural metallic materials, magnesium (Mg) alloys stand out as the lightest, possessing a density of around 1.74 g/cm³. Their lightweight nature makes them approximately 35% less dense than aluminum, offering a significant advantage in applications where reduced mass is crucial.The remarkable low density of Mg alloys, paired with their advantageous specific strength and rigidity, renders them highly desirable for use in aerospace, automotive, biomedical, and electronic applications. Their ability to significantly reduce overall weight makes them an excellent choice for industries where minimizing mass is a priority.. Magnesium exhibits **good castability, machinability, and electromagnetic shielding,** but its relatively low ductility, poor resistance to corrosion, and limited formability at ambient temperature pose challenges for widespread structural use.

Mg alloys are generally categorized into **wrought alloys and casting alloys**, with compositions tailored to enhance specific properties. Frequently used elements in alloy composition include Al, Zn, Mn, Zr, RE (rare earths), Ca, and more recently, Bi, Li, and Sn. For example, the **AZ series (Mg– Al–Zn)** and **AM series (Mg–Al–Mn**) offer good mechanical strength and moderate resistance to corrosion, while the **ZK series (Mg–Zn–Zr)** provides improved toughness and weldability. **RE-containing alloys such as WE43 and AE42 are used in high-temperature applications due to their excellent creep resistance.** Magnesium alloys are characterized by their hexagonal close-packed (HCP) crystal configuration, which inherently restricts the number of slip systems accessible for deformation under ambient conditions.. As a result, deformation occurs mainly through twinning and basal slip, leading to poor ductility and anisotropic mechanical behavior. However, through thermomechanical treatments like hot rolling, extrusion, and annealing, it is possible to refine grains, modify texture, and activate non-basal slip systems to improve ductility and formability. Despite their drawbacks, magnesium alloys continue to evolve through alloy design and process

optimization. Elements such as Li can reduce density further and increase ductility; Ca and Bi enhance corrosion resistance and dynamic recrystallization; and Sn, Zn, and Mn contribute to solid solution strengthening and intermetallic phase formation.

1.2 Frequently used alloying elements in magnesium

Magnesium alloys are typically strengthened and modified through the addition of various alloying elements, each offering unique benefits to microstructural stability, mechanical performance, corrosion resistance, and functional properties. Common alloying elements include zinc (Zn), manganese (Mn),aluminum (Al), rare earth elements (REs), zirconium (Zr), calcium (Ca), tin (Sn), lithium (Li), and more recently, bismuth (Bi).

Aluminum (Al) is the most widely used element in Mg alloys (e.g., **AZ and AM series**), offering good strength through solid solution strengthening and hardening as a result of precipitates. It also enhances castability but can reduce corrosion resistance in chloride-rich environments.

Zinc (Zn) Enhances mechanical durability and resistance to deformation over time, frequently utilized in conjunction with aluminum. It contributes to age hardening and forms secondary phases like MgZn or $MgZn_2$, which refine grain structure and improve mechanical response.

Manganese (Mn) serves mainly as a grain refiner and impurity getter, improving corrosion resistance by reducing iron content in solid solution. It is a critical element in **AM and AZ series alloys.**

Rare Earth Elements (REs) Elements from the Rare Earth group, including Nd, Y, Gd, and Ce, contribute to superior performance at elevated temperatures by enhancing structural integrity, minimizing creep deformation, and improving thermal stability. Additionally, their presence modifies texture characteristics, resulting in increased ductility and better material workability.

Zirconium (Zr) is used primarily in non-Al-containing Mg alloys (e.g., **ZK series**) as a potent grain refiner and recrystallization controller, especially in high-purity systems.

Calcium (Ca) is a lightweight, cost-effective addition that improves creep resistance and ignition resistance, making it suitable for automotive applications. It also modifies the texture and enhances corrosion resistance at low concentrations.

Tin (Sn) enhances mechanical properties through solid solution and precipitation strengthening mechanisms. In minor quantities, it aids in grain refinement, leading to a finer microstructure while simultaneously boosting corrosion resistance.

Lithium (Li) significantly reduces density and increases ductility, especially in dual-phase α+β Mg–Li alloys. It is useful in applications requiring ultra-lightweight, highly formable materials.

Bismuth (Bi), as discussed extensively in this review, enhances grain refinement, promotes dynamic recrystallization, and contributes to superplasticity and electrochemical performance when appropriately alloyed with Mg.

1.3 Structure of Mg alloys

Magnesium in its pure form adopts a hexagonal close-packed (HCP) crystal arrangement, characterized by lattice constants of a = 0.320 nm and c = 0.521 nm, as depicted in Fig 1.1.. The HCP crystal structure is characterized by limited number of slip systems at ambient temperature—primarily the basal <a> slip—making Mg inherently brittle and difficult to deform at ambient conditions. This crystallographic anisotropy is one of the fundamental reasons for the **poor ductility and formability of Mg alloys compared to FCC or BCC metals.**

In the hexagonal close packed (HCP) structure**, only three independent**

slip systems are typically active at room temperature, which is not sufficient to adjust for any arbitrary plastic deformation (as per von Mises criterion). **To overcome this limitation, plasticity in Mg is often aided by twinning, particularly tension twinning along the {10-12} planes.** At elevated temperatures, alternative deformation mechanisms beyond basal slip—such as prismatic and pyramidal slip system play a crucial role in accommodating plastic strain under certain stress conditions because they are being activated, enhancing ductility and formability. Alloying elements and thermomechanical processing (like hot rolling) can significantly influence the activity of these deformation mechanisms. For example, elements like Bi, Ca, or REs can modify texture and promote dynamic recrystallization, thereby altering the mechanical response and improving ductility. Understanding the HCP structure and its implications on deformation behavior is essential for tailoring magnesium alloys for structural applications.

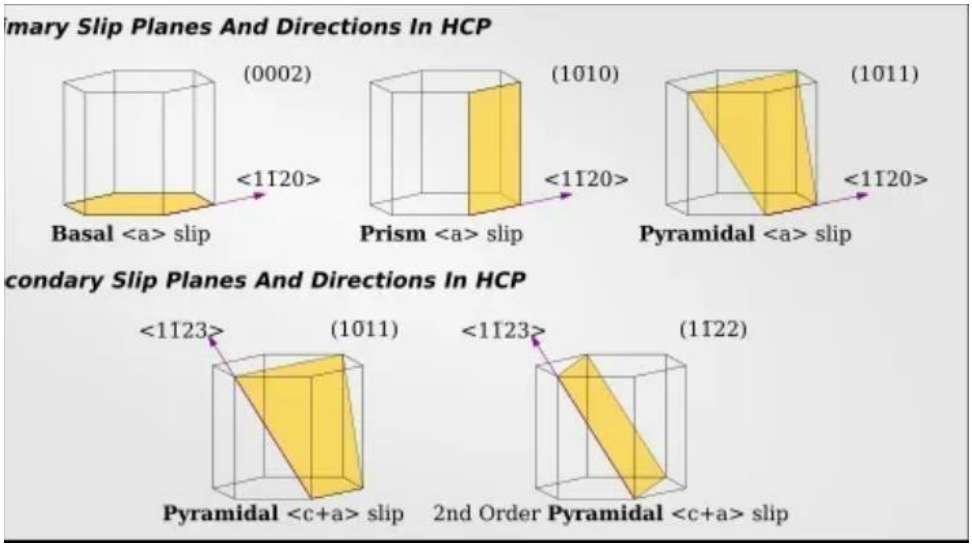

Fig1.1: Shows the hcp crystal structure of Mg and slip planes and directions

1.4 Applications of Mg based alloys

Magnesium-based alloys are valued across industries for being lightweight, strong, and easy to machine.. One of the most prominent applications is in the automotive sector, where Mg alloys are used to make the vehicle lightweight, thereby enhancing the vehicle's fuel efficiency

and decreasing the carbon dioxide (CO_2) emissions of the vehicle.
Components such as Components such as seat frames, engine blocks, transmission casings, and steering wheels as shown in **Fig1.2**.

Fig1.2: Shows the real world use of Mg based alloys in fabricating steering wheels.

Mg based alloys are highly regarded in aerospace applications due to their outstanding balance of strength and lightweight properties, making them an ideal choice for reducing overall structural mass while maintaining mechanical integrity. making them suitable for non-critical structural components, interior fittings, and helicopter gearbox housings. Their use contributes significantly to weight savings and enhanced fuel economy in aircraft.

Mg alloys are also employed in **electronics** for casings in laptops, mobile phones, and cameras due to their EMI shielding properties and ease of die casting.

Furthermore, in the **energy sector**, Mg–Bi and other Mg-based alloys are gaining attention for electrochemical energy storage applications, especially in magnesium-ion batteries,because oftheir high volumetric capacity and favorable alloying behavior.

1.5 Limitations of Mg based alloys

Although magnesium alloys exhibit a favorable combination of low density and high specific strength, several significant drawbacks restrict

their broader adoption across various industries.

Poor Ductility: Due to their crytsalligraphic structure of hexagonal close-packed (HCP) crystal structure, Mg alloys have limited number of active slip systems at ambient temperature, restricting the plastic deformation.

Poor resistance to Corrosion: Mg alloys are highly reactive and prone to galvanic and pitting corrosion, especially in moist or saline environments.

Limited High-Temperature Strength: At elevated temperatures, the mechanical integrity of these alloys deteriorates quickly, limiting their suitability for applications requiring high thermal stability.

Casting and Formability Issues: Conventional casting often leads to defects like porosity and segregation; their poor formability also limits complex shaping.

Texture-Dependent Anisotropy: Strong basal texture formed during processing results in mechanical anisotropy, affecting uniformity in properties.

Weldability Challenges: Mg alloys are difficult to weld due to oxidation and the formation of brittle intermetallic phases.

1.6 Balancing Strength and Ductility in Magnesium Alloys

Magnesium alloys exhibit a classic strength–ductility trade-off, where enhancing one property often leads to the deterioration of the other. This trade-off is fundamentally governed by the principles of mechanical metallurgy:

Grain Refinement and Strengthening: From the Hall-Petch principle, we observe that reducing grain size increases yield strength due to grain boundary strengthening. However, finer grains can also restrict dislocation movement, which limits plastic deformation and reduces ductility.

Precipitation and Second Phase Strengthening: While the introduction of precipitates and secondary phases (e.g., $Mg_{12}Ce$, $Mg_{17}Al_{12}$) impedes dislocation motion and enhances strength, they also act as stress concentrators and crack initiation sites, reducing ductility.

Texture Effects: Strong basal textures developed during rolling or extrusion promote easy slip along the basal plane but restrict deformation in non-basal directions. This anisotropic deformation enhances strength but limits formability and ductility.

Limited Slip Systems: The hexaagonal close packed (HCP) crystal structure associated to Magnesium has lesser number of active slip systems at t h e a m b i e n t temperature, making it hard for the material to accommodate uniform plastic deformation—this inherently restricts ductility.

Need to Overcome the Trade-off

Overcoming the strength–ductility trade-off is essential for the wider adoption of Mg based alloys in structural applications such as transportation, aviation, and medical industries.. Achieving a optimum balance between mechanical strength and ductility **enables improved crashworthiness and energy absorption, enhanced fatigue resistance and structural integrity, greater design flexibility and formability**

Chapter 2

LITERATURE REVIEW

Magnesium (Mg) based alloys have attracted huge amount of interest because of their lightweight nature; but, their restricted ductility at room temperature poses a significant challenge to their broader use. This limitation stems from the few active deformation modes available at ambient conditions. In materials with a hexagonal close-packed (HCP) crystal arrangement like magnesium,the slip behavior exhibits a high degree of anisotropy. The slip occuring on basal plane is the most easily activated because of its low critical resolved shear stress (CRSS), whereas non-basal slip systems require considerably higher CRSS values, making them less effective under typical conditions. A comprehensive understanding and modification of these slip systems are crucial for enhancing the mechanical properties of Mg based alloys. This literature review consolidates essential insights regarding the characteristics, activation, and improvement of both basal and non-basal slip systems as reported in recent studies.

2.1 Basal & Non-basal deformation mode in Mg based alloys

Basal slip in Mg based alloys is the predominant mode of plastic deformation in hexagonal close-packed (HCP) metals like magnesium (Mg)**.** It occurs along the {0001} basal plane in the <11-20> direction, which aligns with the close-packed atomic arrangement**.** Basal slip, occurring on the {0001}<11-20> plane and direction, is the dominant deformation mode in pure Mg due to its low CRSS. Li et al. (2021) found that in Mg–2Y alloys, the require value of CRSS to initiate basal slip is approximately 12.5 MPa as shown in Table 2.1 below[1]. Similar low CRSS values were confirmed by Zhu et al. (2019), Sandlöbes et al. (2011), and Lee et al. (2019), which highlight the ease of basal slip activation in Mg alloys[2,5,7]. While favourable for initiating plastic deformation, the over-reliance on basal slip can hinder ductility due to insufficient

independent slip systems, particularly when a strong basal texture develops during thermomechanical processing (Yan et al., 2013; Lee et al., 2019) [7,8].

TABLE 2.1 Table showing *CRSS* value for different slip modes in Mg–2Y alloy.

Slip Mode	τ_{CRSS}		
	25°C	100°C	250°C
Basal Slip	12.5±1.7	-	-
Twin Nucleation	38.5±1.2	-	-
Twin Growth	33.8±0.7	-	-
Prismatic Slip	-	-	39.7±0.3
Pyramidal slip	-	43.7±0.3	45.6±0.7

Alloys exhibiting a distinct basal texture often restrict deformation to the basal planes, leading to reduced formability. Lee et al. (2019) illustrated that extruded Mg-1Gd alloys, characterized by a rare-earth induced basal texture, showed limited capacity for deformation accommodation [7]. Similarly, Yan et al. (2013) noted that a pronounced basal texture in Mg-2.0Zn-0.8Gd rolled sheets limited slip activity during tensile deformation at ambient temperature[8].

Non-basal modes of slip: Magnesium (Mg) based alloys predominantly deform via basal slip ({0001}<11-20>), which requires a low value of the critical resolved shear stress (CRSS). However, this primary mode has inherent limitations, especially concerning ductility and work hardening,because of the restricted number of independent slip systems which are available. To overcome these constraints, the activation of non-

basal slip systems is essential, as they facilitate additional plastic deformation pathways, leading to more isotropic mechanical behavior. These systems offer the potential for more isotropic plasticity and improved ductility. However, they possess higher CRSS compared to basal slip. As reported by Li et al. (2021), Zhu et al. (2019), and Tang et al. (2024), the typical CRSS for prismatic and pyramidal slip modes ranges between 34–40 MPa.

The activation of non-basal slip systems can be facilitated through alloying. Elements such as yttrium (Y), calcium (Ca), lithium (Li), erbium (Er), samarium (Sm), and manganese (Mn) have been shown to decrease the CRSS gap between the basal and non-basal systems[6]. These solute elements work by decreasing the stacking fault energy (SFE) and promoting more homogeneous deformation. Huang et al. (2018), using the in situ 3D X-ray diffraction, confirmed the occurrence of non-basal slip in Mg-Y alloys as shown in Fig 2.1[3].

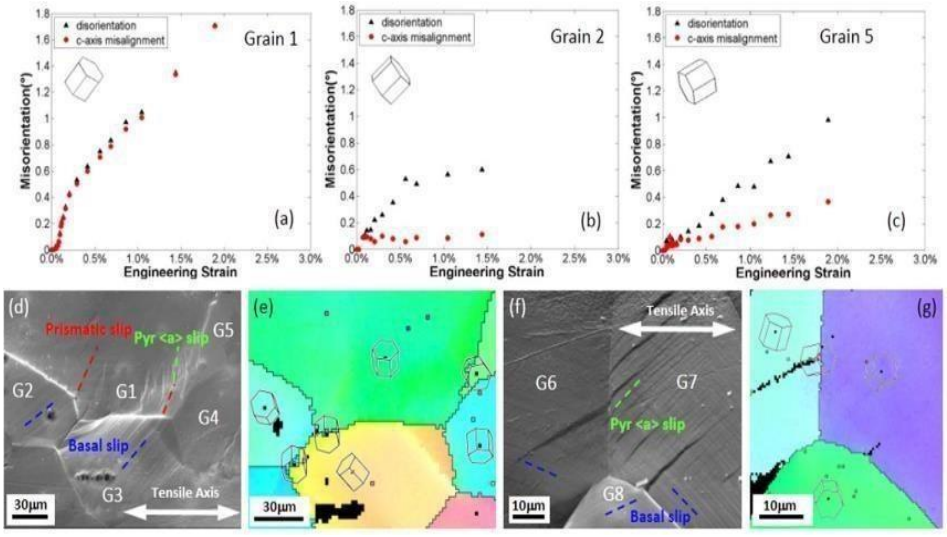

Fig 2.1 :(a–c) Evolution of disorientation and misalignment of c-axis in Grains 1, 2, and 5 during deformation, illustrating grain orientation through a hexagonal prism representation in the top-left corner of each figure, (d–g) Electron Backscatter Diffraction (EBSD)-based slip trace analysis of a specimen deformed separately , showing slip activity across basal, prismatic, and pyramidal systems in distinct grains.

Tang et al. (2024) developed a high-ductility Mg based alloy by co-alloying with Li and Er, which activated non-basal slip and improved intergranular deformation coordination. Their alloy exhibited enhanced plasticity and reduced texture intensity. Zhou et al. (2023) focused on decreasing the strength difference between basal and non-basal slips by targeted alloying strategies, which led to more uniform deformation and improved ductility as shown in Table 2.2.[6] In a follow-up study, Zhou et al. (2024) reported that adding micro-alloyed Mn led to increased activity of non-basal slips and improved strain accommodation in Mg based alloys.

TABLE 2.2 Table showing $\Delta CRSS$ value for different slip systems and effect of alloying on $\Delta CRSS$

Slip Mode	Typical CRSS (MPa)	Effect of Alloying
Basal	12–13	Slight increase
Prismatic	~34–40	Decreased
Pyramidal <c+a>	~34–40	Decreased

The decrease in value of CRSS for non-basal systems with appropriate alloying is essential to their activation. For example, Zhu et al. (2019) showed that the addition of Ca promoted <c+a> pyramidal slip in Mg based alloys, which significantly improved ductility without compromising strength.

Microstructural factors also influence the activation of slip systems. Fine grain size, tailored textures, and the absence of coarse second-phase particles encourage activation of t he non-basal slip systems. Tang et al. (2024) and Zhou et al. (2024) emphasized that microstructural homogeneity is vital for activating multiple deformation mechanisms.

Twinning, particularly {10-12}<10-11> extension twinning, is another critical mechanism of deformation in Mg based alloys. While it helps

accommodate the plastic strain, especially along the c-axis, its interaction with slip modes is complex. Li et al. (2021) and Sandlöbes et al. (2011) demonstrated that twinning often complements non-basal slip in enabling more uniform deformation. Lee et al. (2019) and Yan et al. (2013) showed that alloying and texture control could suppress excessive twinning, allowing for better exploitation of slip-based deformation mechanisms [7,8].

The primary benefit of activating non-basal slip systems lies in the improved ductility and isotropic mechanical behavior they confer. Studies by Sandlöbes et al. (2011), Jang et al. (2021), and Zhou et al. (2023) consistently report enhanced formability and strain hardening behavior in Mg alloys that activate prismatic and pyramidal slips. However, non-basal slip systems are inherently more difficult to activate due to their higher CRSS. The efficacy of alloying depends on precise composition and processing control. Even minor variations can result in large differences in mechanical response [6].

Therefore, the deformation characteristics of magnesium based alloys are influenced by the interplay between basal and non-basal slip mechanisms. While basal slip is readily activated, its predominance can limit ductility. Conversely, non-basal slip mechanisms, although more challenging to initiate, can significantly improve mechanical performance when supported by suitable alloying and microstructural techniques. The reviewed studies indicate that alloying with elements such as Y, Ca, Li, Er, Sm, and Mn effectively narrows the value of CRSS disparity between various slip systems, promoting more uniform deformation. By integrating alloy design, texture optimization, and microstructural enhancement, it is

feasible to create magnesium alloys with enhanced ductility and formability, making them appropriate for structural applications.

2.2 Mg-rare earth alloys vs Mg-non-rare-earth alloys

Recent research has highlighted distinct differences between rare-earth (RE) and non-rare-earth (non-RE) Mg alloys in terms of mechanical behavior, microstructure, corrosion resistance, and cost.

Mechanical Properties: RE elements such as gadolinium (Gd) lead to a five times increase in basal CRSS and an eight times increase in twinning CRSS (Zhu et al., 2019). These increases enable better strength and ductility by promoting dislocation interactions and suppressing twin formation. Non- RE alloys (e.g., Mg-Al, Mg-Ca, Mg-Zn systems) improve strength modestly but do not achieve the same level of enhancement in ductility or slip system activity.

Microstructure: RE elements form short-range ordered (SRO) clusters, as observed by Sandlöbes et al. (2011) and Huang et al. (2018), which interact with dislocations and influence slip and twinning mechanisms[3]. Such microstructural features are largely absent in non-RE systems, which limits their impact on CRSS and ductility enhancement.

Corrosion Resistance: Zhu et al. (2019) noted that RE elements tend to improve corrosion resistance, though this effect is alloy-specific. Non-RE elements like Ca and Zn offer mixed corrosion behavior, often requiring protective coatings or careful processing.

Cost and Availability: RE elements are expensive and scarce, making them less viable for large-scale applications. Non-RE alloying elements are more abundant and cost-effective, favoring automotive and general industrial use (Zhou et al., 2023).

Applications: The choice of alloying strategy depends on performance versus cost. Mg-RE a l lo ys are preferred for aerospace and high-

performance structural applications, while Mg-non-RE alloys are chosen for cost-sensitive, mass-manufactured components.

TABLE 2.3 Table showing the comparison between Mg-RE alloys and Mg-non RE alloys in terms of strength and ductility, microstructure, cost and availability, and applications

Alloy Type	Strength & Ductility	Microstructure Effects	Cost & Availability	Typical Applications
Mg-RE Alloys	Significantly higher; improved by SRO clusters	Unique SRO clusters, enhanced slip/twinning	High cost, limited supply	Aerospace, high-performance
Mg-non-RE Alloys	Improved, but less than RE	Standard microstructural changes	Cost-effective, abundant	Automotive, general use

2.2.1 Reason for choosing Mg-Bi instead of Mg-RE alloys

Magnesium-rare earth (Mg-RE) alloys have shown exceptional mechanical performance, particularly at high temperatures. However, their high cost and limited global availability pose significant challenges. In contrast, magnesium-bismuth (Mg-Bi) alloys are emerging as promising alternatives because of their cost-effectiveness and comparable mechanical properties. The study by Tang et al. in 2023 highlighted these advantages, noting that Mg- Bi alloys can offer competitive performance while significantly reducing material costs.

Mechanical Properties comparison:

Mg-RE alloys benefit from the addition of elements like gadolinium (Gd), yttrium (Y), and neodymium (Nd), which lead to substantial increases in strength and ductility. The research conducted by Tang et al. in 2023 demonstrated that alloys such as Mg-17Gd-0.5Zr and Mg-10Gd-5Y-0.4Zr achieved yield strengths of 278 MPa and 289 MPa, respectively. These improvements are largely due to solid solution strengthening and the

formation of thermally stable intermetallic phases, which inhibit dislocation motion and thus enhance mechanical properties, especially at high temperatures.

In comparison, Mg-Bi alloys utilize the limited solid solubility of bismuth in magnesium to form fine Mg_3Bi_2 precipitates. These precipitates contribute to strengthening through dispersion hardening. The study by Xue et al. in 2017 found that an as-extruded AZ80-2Sn-0.5Bi alloy exhibited a yield strength of 247.1 MPa and an ultimate tensile strength of 379.6 MPa. Similarly, research by Wang et al. in 2011 on AZ81 alloys with 1 wt.% Bi reported enhanced strength due to a refined and uniformly distributed β- $Mg_{17}Al_{12}$ phase.**Nie et al. (2021)** explored the **unusual segregation behavior of Bi** at coherent twin boundaries (CTBs) and found that, contrary to conventional solute segregation models, Bi **segregates at compression sites rather than tension sites as shown in Fig 2.2[19]**. This behaviour, influenced by **chemical bonding rather than strain minimization**, contributes to **stabilizing the grain boundaries and enhancing mechanical stability during plastic deformation**. This segregation behavior plays an important role in controlling the recrystallisation process during hot rolling leading to improved texture and mechanical properties.

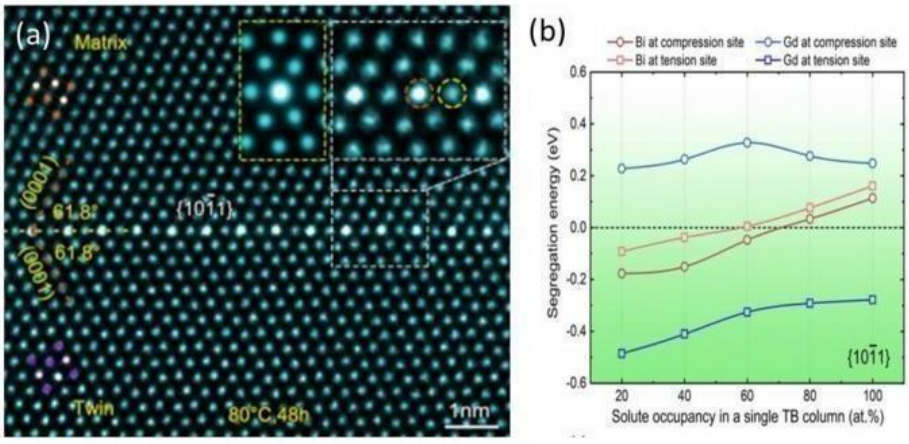

Figure 2.2: (a) High angle annular dark field image showing Bi segregation at compression twin boundaries rather than tension twin boundaries, (b) Segregation energy calculations at different solute occupancies.

Thermal Stability comparison:

Mg-RE Alloys: Thermal performance is a critical consideration for high-temperature applications. Dong et al., in their 2020 study, showed that Mg- RE alloys can retain their mechanical strength up to 300°C because of the stability of rare earth-containing intermetallic phases.

Mg-Bi Alloys: Mg-Bi alloys, meanwhile, offer excellent thermal stability through the formation of the Mg_3Bi_2 phase, which remains stable up to 821°C. **Somekawa et al. (2018)** demonstrated that Bi enhances **room-temperature deformability and energy absorption** by promoting **grain boundary sliding (GBS)**, which contributes to an approximately **70% increase in elongation** compared to conventional Mg alloys[18]. The study revealed that Bi does not segregate at grain boundaries but forms **precipitates (Mg3Bi2)**, leading to the formation of **equilibrium grain boundaries**, which are beneficial for deformation processes such as hot rolling because the **Mg3Bi2 precipitates are thermally stable at higher temperatures as shown in Fig 2.3**. The investigation by Yuan et al. in 2022 revealed that this thermal stability contributes to improved resitance to creep and fracture strength at high temperatures, making Mg- Bi alloys suitable for engine and powertrain components.

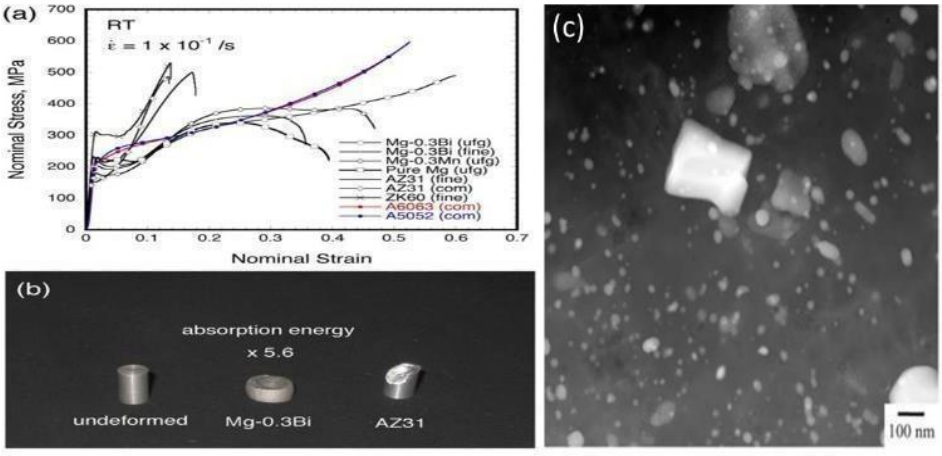

Figure 2.3:(a) Stress versus strain curves of Mg-Bi alloys vs conventional Mg alloys, (b) Compression test results showing barrel-shaped deformation in Mg-Bi alloy,(c) ADF-STEM image showing dispersed Mg_3Bi_2 precipitates.

Microstructure and Strengthening Mechanisms comparison:

The study by Wang et al. in 2022 examined the effect of Bi on the microstructural evolution of Mg-Bi alloys and reported that Bi promotes dynamic recrystallization (DRX), leading to grain refinement and a favorable basal texture. These microstructural modifications enhance both strength and ductility. Furthermore, the incorporation of secondary elements such as Ca and Mn into Mg-Bi alloys improves precipitate distribution and morphology, as discussed in Tang et al.'s 2023 review. This synergistic refinement further boosts the mechanical performance of the alloy.Recently, **He et al.** carried out a study on **cold-deformed Mg-3wt%Bi alloy,** focusing on the **occurrence of stacking faults and partial dislocations associated with the deformation as shown in Fig 2.4.** Their findings identified different types of stacking faults and explained their formation mechanisms. This explanation was further validated through molecular dynamics simulations, providing deeper insight into the deformation behavior of Mg-Bi alloys.

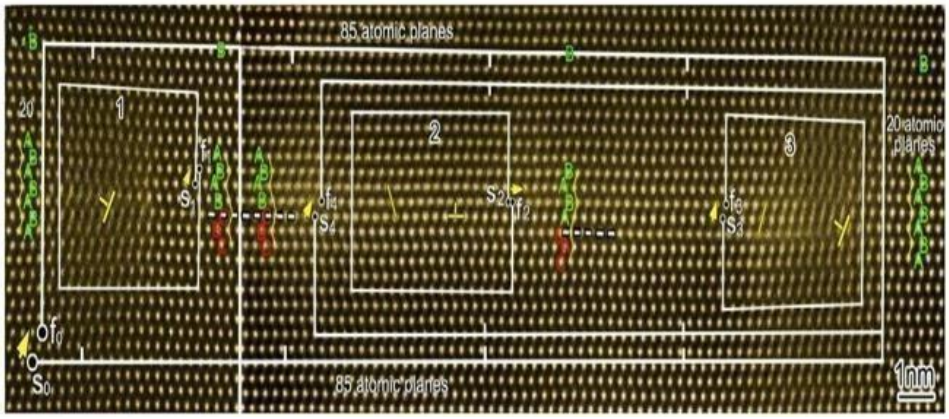

Figure 2.4:HAADF-STEM images revealing the unexpected presence of Shockley partial dislocations within I1 stacking faults, facilitating enhanced ductility and plastic deformation in the Mg-Bi alloy.

Cost and Availability comparison:

The economic and supply considerations of rare earth elements present a significant limitation for the wide-scale adoption of Mg-RE alloys. Tang et al. in their 2023 review emphasized that the cost and limited availability of RE elements such as Gd and Y constrain their industrial application. Conversely, bismuth is more abundant and cost-effective, making Mg-Bi alloys an attractive option for automotive and general engineering sectors where performance must be balanced with cost efficiency.

TABLE 2.4: Table showing comparison of Mg-Bi alloys and Mg-RE alloys in terms of cost, strengthening method, microstructure control and availability

Feature	Mg-Bi Alloys	Mg-RE Alloys
Cost	Lower	Higher (due to RE)
Strengthening Method	Bi precipitates	RE precipitates
Microstructure Control	Enhanced with Ca, Mn	Inherent with RE
Availability	More accessible elements	Limited by RE supply

2.3 Role of Bismuth (Bi) as an alloying element

Among structural metals, magnesium (Mg) holds the distinction of being the lowest in density, and is extensively studied for automotive, aerospace, and electrochemical energy storage applications. However, challenges like poor value of ductility, less corrosion resistance, and inadequate electrochemical properties have limited its commercial utility. Bismuth (Bi), as a low-melting-point, non-toxic element with a high atomic number, has shown significant potential to address these limitations. Recent research has explored Bi's influence on microstructural evolution, mechanical properties, and electrochemical performance, particularly in Mg-based alloys.

Effect of Bismuth (Bi) on Microstructural Evolution and Mechanical Properties

Grain Refinement: The study by Joshi and Babu in 2015 revealed that the addition of as little as 0.2 wt% Bi to AZ31 Mg alloy resulted in an up to 50% decrease in average grain size. This refinement of grains occurred independent of the cooling rate, indicating that Bi effectively stabilizes the microstructure during solidification. The refined grain structure leads to more homogeneous deformation and improved mechanical isotropy.

Morphology Modification: The research conducted by Erjun et al. in 2008 found that Bi addition significantly altered the morphology of the Mg2Si intermetallic phase. Specifically, the optimal Bi content (0.5 wt%) transformed the coarse dendritic Mg_2Si particles into fine, polyhedral shapes, which enhanced the mechanical interaction between the primary Mg matrix and the intermetallics. However, they also noted that Bi content above 0.8 wt% reversed this beneficial effect, leading to coarser dendritic morphologies that degraded mechanical properties.

Ductility and Deformability: The study by **Somekawa et al. in 2018** demonstrated that **Mg-Bi alloys exhibit excellent room-temperature deformability**. In particular, elongation-to-failure values reached up to 170%, showcasing superplastic-like behavior. **The ductility was attributed to enhanced grain boundary sliding facilitated by fine equiaxed grains and low texture intensity.** Complementing this, the work by Somekawa and Singh in 2018 confirmed that dilute Bi additions promoted superior room-temperature ductility by enabling more effective grain boundary sliding mechanisms.

Dynamic Recrystallization(DRX) Behavior: **Yu et al. in 2021** conducted a comprehensive investigation into the dynamic recrystallization (DRX) behavior of Mg alloys containing 3 wt% Bi[22]. Their results showed that **Bi promotes DRX by accelerating grain boundary mobility and nucleation of new grains during thermomechanical processing.** The refined grains and enhanced DRX

contribute to increased formability and reduced flow stress at elevated temperatures.

2.3.1 Properties of Bi and Its Solubility in Mg

Among the various alloying elements, bismuth (Bi) has attracted attention for its ability to form **stable intermetallic phases** with magnesium, thereby influencing mechanical strength, ductility.

Solubility and Intermetallic Phase Formation:

Bismuth exhibits **moderate solubility** in magnesium, which facilitates the formation of various intermetallic phases. The solubility limit of Bi in Mg allows for the formation of stable binary compounds, particularly under processing conditions such as hot extrusion.

Go et al. (2020) found that the addition of 6–9 wt% Bi to Mg resulted in the **precipitation of fine Mg_3Bi_2 particles during hot extrusion**. **These fine precipitates confirm a significant solubility and high reactivity between Bi and the Mg matrix[23].**

Chen et al. (2022), using first-principles calculations, identified several mechanically and dynamically stable intermetallics in the Mg-Bi binary system: **Mg_3Bi_2, Mg_4Bi, Mg_3Bi, Mg_2Bi, and MgBi. Among these, Mg_3Bi_2 is the most studied and stable phase.These intermetallic compounds form readily during solidification or thermo-mechanical processing, suggesting that Bi has a high affinity for Mg and a propensity to form strengthening precipitates[24].**

2.3.2 Effect of Bi on microstructure & Precipitate Formation

Bismuth (Bi) addition to magnesium (Mg) alloys has been comprehensively studied due to its significant influence on microstructure evolution, precipitate formation, and the resultant mechanical and corrosion properties. These effects are highly dependent on Bi concentration, alloy system, and thermomechanical processing conditions.

This review synthesizes recent studies to provide a thorough understanding of how Bi modifies the microstructure and contributes to strengthening mechanisms in Mg-based alloys.

Microstructure Refinement: Bi plays a crucial role in refining the grain structure of Mg alloys. The **formation of Mg3Bi2 precipitates**, **facilitated by Bi additions, acts as effective nucleation sites during recrystallization and dynamic recovery, particularly during the hot extrusion processes.** Guo et al. (2024) demonstrated that in Bi-modified Mg alloys, grain sizes could be refined to as small as ~80 nm at lower extrusion temperatures. These ultra-fine grains are attributed to the dynamic precipitation of nano-sized Bi-rich clusters which inhibit grain growth[21].

Similarly, **Tok et al. (2015)** observed substantial grain refinement in Mg-1.2Ca-xBi alloys[28]. They reported that **small Bi additions (up to 0.5 wt.%) led to fine and equiaxed grains, enhancing the corrosion resistance and mechanical properties**. **However, higher Bi content induced grain coarsening due to excessive formation of secondary phases.**

Precipitate Formation: The nature and morphology of precipitates are heavily influenced by Bi content. **At low Bi levels (≤0.5 wt.%), fine Mg3Bi2 precipitates are primarily observed. These precipitates contribute to grain refinement, precipitation hardening, and improved corrosion behavior[28].** In Mg-Zn-Co alloys, Bi facilitates the formation of strengthening β_1' rod-shaped precipitates along with Mg3Bi2, enhancing the age-hardening response (He et al., 2020).At moderate Bi additions (1.5– 3 wt.%), further evolution of secondary phases occurs, including Mg2Ca and complex Bi-containing intermetallics such as Mg2Bi2Ca. Tok et al. (2015) reported that although strengthening effects increase at this range, microstructural coarsening becomes more pronounced, potentially affecting ductility and corrosion performance[28].For high Bi content (≥5 wt.%),precipitates tend to

coarsen and increase in volume fraction, which can lead to galvanic corrosion because of the strong electrochemical potential difference between Mg and intermetallics[28]. Coarser precipitates also reduce the effectiveness of grain boundary pinning, undermining the refining benefits.

Thermal Stability and Strengthening Effects:Yuan et al. (2001) emphasized the **thermal stability of Mg3Bi2 precipitates, indicating their potential to suppress undesirable discontinuous precipitation,** which often degrades mechanical performance at elevated temperatures[26]. **These thermally stable particles also enhance creep resistance by providing a strong pinning effect on grain boundaries.**Guo et al. (2024) further confirmed that nano-sized Bi-rich clusters forming during hot extrusion contribute to significant strengthening through Orowan looping and grain boundary stabilization[27]. These effects are synergistic with the reduced grain size, providing a dual mechanism of strengthening.

Corrosion Behavior: The corrosion behaviour of the Mg based alloys is sensitive to Bi content. Tok et al. (2015) and Bakhsheshi-Rad et al. (2017) observed that **low Bi additions (≤0.5 wt.%) improve corrosion resistance due to the formation of fine, uniformly distributed Mg3Bi2 particles that limit galvanic interactions**[28]. However, as Bi content increases, galvanic coupling between the matrix and Bi-rich intermetallics becomes more pronounced, leading to accelerated degradation.

2.3.3 Influence of Bi on the mechanical Properties

Microstructure Refinement and Dynamic Recrystallization: Bi plays a crucial role in refining the grain structure of Mg alloys. The formation of Mg_3Bi_2 phases, facilitated by Bi additions, acts as effective nucleation

sites during the recrystallization process and dynamic recovery. Guo et al. (2024) demonstrated that extrusion temperature significantly influences the distribution of Bi clusters and grain refinement, with ultra-fine grains (~80 nm) forming at lower extrusion temperatures due to Bi-induced dynamic precipitation.Yu et al. (2021) further reported that a 3 wt.% Bi addition to a Mg alloy promotes dynamic recrystallization (DRX), where Bi clusters located at grain boundaries serve as the nucleation sites[35]. The DRX fraction increased with temperature, resulting in improved grain refinement and uniformity.

Strength and Ductility: Bi additions at low to moderate levels improve both tensile strength and ductility. **Wang et al. (2011) found that in AZ80 alloys, tensile strength and elongation peaked at 0.5 wt.% Bi, reaching 283 MPa and 9.2%, respectively[31].** This improvement is **because of grain refinement and the precipitation of finely dispersed Mg_3Bi_2 phases.**However, excessive Bi (>1 wt.%) can reduce mechanical performance. Xing-Yuan (2010) and Li et al. (2011) noted that **high Bi levels lead to the formation of coarse Mg_3Bi_2 particles, which split the matrix and reduce both strength and ductility due to interfacial debonding.** Li et al. (2011) found that AZ81 alloys with 1.5 wt.% Bi exhibited reduced elongation (~6%) due to the coarse intermetallics[37].

High-Temperature Strength and Creep Resistance: Zheng-Hua (2013) and Yuan et al. (2001) emphasized the role of Bi in enhancing high-temperature strength and creep resistance[30,32]. **Mg_3Bi_2 phases are thermally stable, preventing grain boundary sliding and suppressing discontinuous precipitation** during prolonged exposure to elevated temperatures. Xing-Yuan (2010) noted that Bi-containing AZ81 alloys exhibited higher yield strength at 150 °C compared to Bi-free variants.

Superplastic Deformability: Somekawa & Singh (2018) and Somekawa et al. (2018) demonstrated exceptional superplasticity in dilute Mg-Bi binary alloys[33,34]. A Mg-0.3 at.% Bi alloy achieved room-temperature

elongation up to 170% at a strain rate of 3×10^{-4} s^{-1}. This is linked to grain boundary sliding facilitated by uniform, ultra-fine grains and Bi-segregation at grain boundaries, which enhances grain boundary mobility.

2.3.4 Literature Basis for Selecting 0.4 wt% Bi Composition

Corrosion Resistance and Electrochemical Performance: A primary motivation for incorporating Bi into Mg based alloys is to improve resistance to corrosion , particularly in chloride-containing environments. Wu et al. (2020) investigated the performance of Mg–8Al–0.4Bi alloys in NaCl solution and found that this specific composition exhibited superior corrosion resistance and higher utilization efficiency compared to both lower and higher Bi concentrations. The enhancement is attributed to the formation of Mg17Al12 and BiOCl phases during discharge, which act synergistically to reduce corrosion rates and improve electrochemical behavior. Notably, these phases stabilize the passive layer and inhibit localized degradation.

Similarly, Tok et al. (2015) analyzed the corrosion behavior of Mg–1.2Ca–xBi alloys with varying Bi contents (0.4 to 12 wt%) and found **that the alloy containing 0.4 wt% Bi demonstrated the lowest corrosion rate. Increasing Bi beyond this threshold led to accelerated degradation[28].** The optimal performance at 0.5 wt% Bi aligns with Wu et al.'s findings and underscores the importance of a controlled Bi concentration.

Microstructural Effects and Phase Formation: **Tok et al. (2015) noted that the addition of 0.5 wt% Bi resulted in Mg3Bi2 phase, which is well-dispersed and contributes to improved corrosion resistance[28].** This concentration effectively refines the **grain structure without promoting excessive formation of cathodic secondary phases.At higher Bi contents (e.g., 3–5 wt% or more), Tok et al. observed the emergence of complex intermetallics such as Mg2Bi2Ca[28]. These phases create strong galvanic coupling with the Mg matrix, leading to micro-galvanic corrosion and a net reduction in the corrosion resistance. In**

contrast, lower Bi levels (<0.4 wt%) failed to generate a sufficient volume fraction of corrosion-inhibiting phases and did not achieve the desired microstructural refinement, indicating suboptimal performance.

Mechanical Properties and Ductility: The mechanical performance of Mg based alloys is also sensitive to Bi content. Somekawa and Singh (2018) studied dilute Mg–Bi binary alloys and found that **an addition of approximately 0.3 at.% Bi (comparable to ~0.4 wt%) led to superior ductility due to enhanced grain boundary sliding.** This effect is tied to microstructural homogeneity and the controlled presence of Bi at grain boundaries, which facilitates deformation without embrittlement.

In contrast, higher Bi additions degrade mechanical properties. Tok et al. (2015) observed that **elevated Bi content resulted in the formation of coarse and brittle intermetallics, which negatively affected ductility and promoted cracking as shown in Table 2.5[28].** These findings establish that the window around 0.4–0.5 wt% Bi not only supports corrosion resistance but also preserves or enhances mechanical integrity.

Feasibility of Other Bi Compositions:The feasibility of using Bi concentrations lower or higher than the 0.4–0.5 wt% range has been critically evaluated. Wu et al. (2020) and Tok et al. (2015) reported that **contents below 0.4 wt% fail to induce significant phase formation or microstructural refinement, resulting in limited improvement in** corrosion resistance and mechanical properties[28].Meanwhile, concentrations above this range tend to form excessive intermetallics such as Mg2Bi2Ca, which exacerbate galvanic corrosion and reduce ductility.

TABLE 2.5: Table showing the comparison between influence of Bi content on corrosion resistance,mechanical properties,microstructure and feasibility

Bi Content (wt%)	Corrosion Resistance	Mechanical Properties	Microstructure/Phases	Feasibility/Drawbacks
<0.4	Limited improvement (Wu et al., 2020; Tok et al., 2015)	May not optimize ductility (Somekawa & Singh, 2018)	Insufficient phase formation (Tok et al., 2015)	Suboptimal property enhancement
0.4–0.5	Optimal improvement (Wu et al., 2020; Tok et al., 2015)	Enhanced ductility (Somekawa & Singh, 2018)	Refined, beneficial phases (Wu et al., 2020; Tok et al., 2015)	Most feasible for applications
>0.5	Decreased, more corrosion (Tok et al., 2015)	Reduced ductility (Somekawa & Singh, 2018; Tok et al., 2015)	Excessive secondary phases (Tok et al., 2015)	Accelerated degradation, brittleness

2.4 Combined Thermal and Mechanical Treatment of Mg alloys

By integrating deformation with heat treatment, TMP facilitates grain refinement, texture optimization, and improved strength and ductility, thereby increasing the applicability of Mg alloys in structural and biomedical fields.

Mechanisms of Thermomechanical Processing:

Dynamic Recrystallization (DRX): TMP, like as high temp rolling,extrusion, forging, promotes DRX, leading to fine, uniform grains and improved mechanical properties. The combination of extrusion and forging results in more intense grain refinement and higher strength and ductility compared to single processes.

Particle-Stimulated Nucleation: Precipitation of secondary phases (e.g., rare earth intermetallics, β-Mg17Al12) during TMP can stimulate DRX, further refining grains and weakening texture, which enhances ductility.

Texture Control: TMP, especially when combined with techniques like pre-twinning or severe plastic deformation, can alter the strong basal texture typical of Mg based alloys, improving room temperature formability.

Influence on the Microstructural evolution and Mechanical Properties:

Grain Refinement: Deng et al. (2023) and Maleki et al.(2023) found that TMP methods such as fast rolling with large thickness reduction, multi- directional forging produce fine or bimodal grain structures, which are linked to higher strength and ductility[41].

Strength and Ductility: Deng et al. (2023) found that Enhanced mechanical properties are achieved through a combined effect of grain refinement, precipitation hardening, and texture modification[41]. For example, multi-directional forging and peak aging can yield ultimate tensile strengths above 370 MPa and elongations near 20%

Superplasticity: Savaedi et al. (2023) observed that Fine-grained Mg alloys processed by TMP can exhibit superplastic behavior, especially when stable intermetallic particles are present to prevent grain growth at high temperatures

2.4.1 Cold vs Hot Rolling

Rolling is a fundamental thermomechanical processing technique widely used to shape metals and manipulate their microstructures. It is primarily classified into two categories: hot rolling and cold rolling, each with distinct temperature regimes, advantages, and metallurgical implications.

Hot Rolling as shown in Fig 2.5 is performed at temperatures above the metal's recrystallization temperature. This allows for dynamic recovery and recrystallization during deformation, resulting in refined grains, homogenized microstructure, and elimination of casting defects. It is typically used for primary breakdown of cast ingots and initial microstructure control.

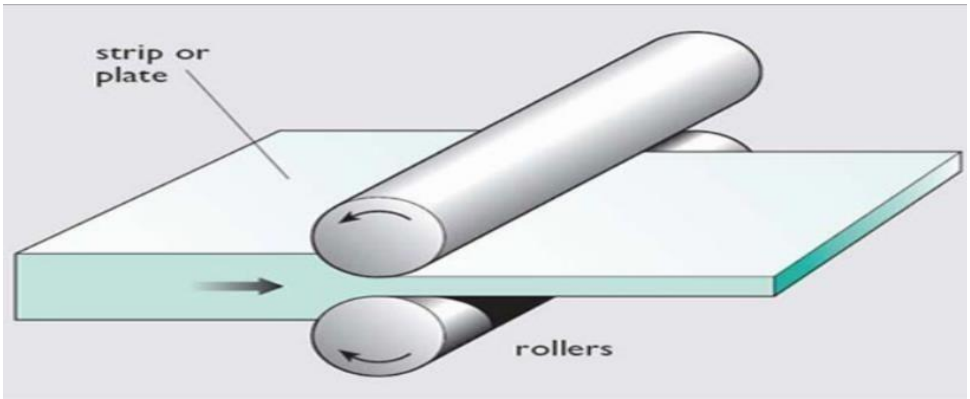

Fig 2.5:Schematic of Hot Rolling

Cold Rolling, in contrast, is carried out below the recrystallization temperature. This process leads to increased dislocation density, higher strength due to work hardening, and improved surface finish, but at the cost of reduced ductility unless followed by annealing.

Table 2.6: comparison of hot rolling and cold rolling based on various parameters.

Parameter	Hot Rolling	Cold Rolling
Temperature Range	Above recrystallization (~0.4Tm or higher)	Below recrystallization
Grain Structure	Recrystallized, refined grains	Elongated grains, higher dislocation density
Strength	Moderate to good	High (due to work hardening)
Ductility	High	Low (unless annealed)
Surface Finish	Moderate	Excellent
Key Application Stage	Initial processing	Final thickness reduction, property tuning

Influence on Microstructure evolution and Mechanical Properties

Hot rolling has been shown to significantly improve microstructural homogeneity and ductility in various alloys. For example, Wei et al. (2024) reported that hot rolling of Ti2AlNb alloys resulted in a refined and equiaxed grain structure that enhanced elongation. Similarly, Liao et al. (2025) observed improved strength-ductility synergy in Fe-based medium entropy alloys (MEAs) processed via single-step hot rolling.

In copper, Ye et al. (2023) found that **hot rolling eliminated porosity in cold-sprayed deposits and increased tensile strength.** For aluminum alloys like AA5083, Algendy et al. (2024) demonstrated that hot rolling at lower temperatures preserved finer grains and increased yield strength.

In contrast, **cold rolling leads to high dislocation density and strengthens metals through work hardening**. Liu et al. (2023) showed that in ferritic stainless steels, cold rolling refined the microstructure and increased strength while improving grain orientation for formability[45]. However, Wei et al. (2024) noted that cold rolling initially reduced ductility before a partial recovery at higher reduction levels.Furthermore, He et al. (2015) revealed that altering cold rolling direction relative to hot rolling can manipulate crystallographic texture—an important consideration for electrical steels.

Advantages and Disadvantages of hot rolling and cold rolling

Hot Rolling Benefits:

Dynamic recrystallization and grain refinement

Improved ductility and elongation

Reduced porosity and homogenized microstructure

Hot Rolling Drawbacks:

Oxidation and scaling at high temperatures

Lower surface finish quality compared to cold rolling

Cold Rolling Benefits:

High strength via work hardening

Excellent dimensional control and surface finish

Enhanced texture and formability post-annealing

Cold Rolling Drawbacks:

Reduced ductility and increased internal stress

May require subsequent annealing to restore formability

Reason for choosing Hot rolling instead of Cold rolling:

The selection of hot rolling in this study is guided by fundamental metallurgical considerations as mentioned below:

Magnesium's HCP Structure and Poor Room-Temperature Ductility: **Because of the limited number of active slip systems in hexagonal close-packed (HCP) structure of magnesium, cold working often results in early crack initiation and limited formability.** Hot rolling, by promoting dynamic recrystallization, enhances ductility and allows for more effective deformation.

Phase Distribution and Grain Refinement: Hot rolling aids in dispersing intermetallic phases like Mg3Bi2, which can enhance strength without severely compromising ductility if controlled properly.

Texture Control: Hot rolling at elevated temperatures provides opportunities to control basal texture, which is critical in determining the anisotropic mechanical behavior of Mg alloys.

Minimization of Work Hardening and Internal Stresses: Avoiding cold rolling at early stages helps reduce residual stresses and internal defects, thereby improving overall mechanical integrity.

2.4.2 Reason for choosing 300°C as Rolling Temp

Hot rolling of Mg-Bi (and similar Mg-based) alloys at 300°C is beneficial because it provides an **optimal balance between strength and ductility.** This temperature allows for significant thickness reduction while maintaining desirable mechanical properties.

Mechanical Properties at 300°C

Strength-Ductility Balance: Rogachev et al.(2024) found that **Hot**

Rolling at 300°C results in a high yield stress (285 MPa), ultimate tensile strength (310 MPa), and moderate elongation (5%)[46]. This combination is considered optimal for many applications, as it provides both strength and some ductility.

Comparison to Higher Temperatures: Rolling at 400°C increases ductility (elongation up to 17%) but reduces strength (yield stress drops to 200 MPa, ultimate tensile strength to 260 MPa). Thus, 300°C is preferred when higher strength is required.

Effects on Microstructure

Recrystallization: At 300°C, the alloy undergoes partial recrystallization, which refines the grain structure and enhances mechanical properties. At 400°C, full recrystallization occurs, leading to lower strength but higher ductility.

Corrosion Resistance

Corrosion Performance: Alloys rolled at 300°C and then heat-treated **show low corrosion rates**, which is important for applications where durability in corrosive environments is needed

TABLE 2.7: Table showing the comparison between hot rolling at 300°C and 400°C in terms of yield strength,UTS,%elongation.

Mechanical Properties of Mg Alloy Rolled at Different Temperatures

Rolling Temp (°C)	Yield Stress (MPa)	Ultimate Tensile Strength (MPa)	Elongation (%)
300	285	310	5
400	200	260	17

Hence ,Hot rolling Mg-Bi alloys at 300°C is necessary and beneficial because it achieves a superior balance of strength and ductility, maintains a refined microstructure, and supports good corrosion resistance. This makes 300°C an optimal processing temperature for applications requiring both mechanical performance and durability.

2.4.3 Overview of influence of hot rolling on microstructure evolution

Hot rolling, a widely utilized thermo-mechanical processing technique, plays a critical role in tailoring the microstructural evolution and mechanical properties of metallic materials. Performed at temperatures above the recrystallization temperature, hot rolling induces significant plastic deformation that drives key metallurgical transformations such as dynamic recovery, dynamic recrystallization, grain refinement, texture development, and phase evolution. These phenomena are highly dependent on the rolling parameters, alloy chemistry, and presence of reinforcements or secondary phases.

1. **Dynamic Recovery and Recrystallization**

At elevated temperatures, hot rolling activates dynamic recovery (DRV), a process that rearranges and annihilates dislocations, leading to a reduction in stored strain energy. This mechanism is particularly dominant in materials with high stacking fault energy (SFE) like aluminum alloys. On the other hand, in alloys with lower SFE such as magnesium or some steels, dynamic recrystallization (DRX) becomes the dominant mechanism, resulting in the nucleation and growth of new strain-free grains[47] .

Liu and Lin et al.,(2003) presented a detailed model for microstructural evolution during multipass hot rolling, capturing the kinetics of DRX and the associated changes in grain structure[47]. They demonstrated that higher temperatures and strains promote DRX over DRV, leading to significant grain refinement and restoration of workability. Tayyebi and Derakhshani Molayousefi et al., (2023), in their review of rolling effects

on high- entropy alloys, highlighted how hot rolling followed by annealing could stabilize refined grains and reduce internal stresses, enhancing mechanical stability.

2. Grain Size Evolution

The evolution of grain size during high temperature hot rolling is governed by a competition between DRX-induced refinement and thermally driven grain growth. The outcome depends on strain rate, temperature, and alloy composition. Wang et al. (2006) developed a physically based model for predicting how grain size evolution occurs during high temperature hot rolling. Their results indicated that increasing temperature and strain rate facilitates finer grain structures, provided that grain growth during inter- pass heating is controlled.

Frazier et al. (2024), using a coupled Potts model–finite element method, simulated the grain size evolution in U-10Mo fuel foils.[48] Their study revealed that the multi-stage hot rolling process led to inhomogeneous microstructures, with grain size ranging from sub-micron to several microns, governed by local strain distribution and phase behavior. Similarly, Cui et al. (2022) introduced a machine learning-based framework that accurately predicted grain size during hot strip rolling by integrating process parameters and material responses[49]. They demonstrated that specific rolling conditions could be optimized to achieve grain sizes within the desired 10–50 μm range.

3. Texture Development

Texture development is a hallmark of hot rolling. As deformation proceeds, grains tend to align along specific crystallographic directions, resulting in preferred orientation. Ghazanlou et al. (2021) studied Al7075 composites reinforced with graphene and carbon nanotubes. They observed elongated grains aligned along the rolling direction and partial recrystallization near the reinforcements, which modified the typical rolling texture. The presence of reinforcements disrupted the

uniform deformation, promoting heterogeneous texture zones. Han et al. (2023) explored the texture evolution in a hot-rolled Mg-3Gd alloy. They showed that increasing rolling strain transformed the microstructure from twin-dominated to shear band-dominated regimes. Upon annealing, weak basal textures formed due to discontinuous DRX, which helped improve formability.

4. Influence of Rolling Parameters on Microstructural Features

Rolling parameters such as temperature, strain rate, rolling reduction, and schedule critically influence microstructure. For instance, higher rolling temperatures promote DRX and grain refinement, but also risk grain coarsening if the temperature is excessive or inter-pass times are long[. Rolling reduction per pass affects the distribution of strain and hence the nucleation sites for DRX[48].

Ghazanlou et al. (2021) found that in their Al7075 hybrid composites, a rolling reduction of 50% at 500 °C led to significant grain refinement and altered texture. Similarly, in the study by Han et al. (2023), a rolling strain of 1.2 followed by annealing at 400°C resulted in 65% recrystallized grains with equiaxed morphology.

Cui et al. (2022) highlighted that through machine learning models, critical rolling force and temperature combinations could be predicted to optimize grain refinement[49]. They suggested that temperatures in the range of 900– 950 °C and moderate strain rates (~0.5–1 s^{-1}) are effective for steels to produce fine grains and uniform textures.

5. Heterogeneity and Modeling of Microstructure Evolution

Microstructural heterogeneity arises due to uneven deformation, phase interactions, and reinforcement distribution. Szeliga et al. (2022) developed a stochastic model to describe microstructural evolution during hot rolling of steel. Their results showed significant variation in grain size and recrystallization across the rolled strip, influenced by thermal gradients and phase fractions.Frazier et al. (2024) used a spatially

resolved simulation approach, revealing that in U-10Mo alloys, heterogeneous strain distribution caused variation in recrystallization and grain boundary migration, affecting fuel performance. These studies underscore the necessity for robust predictive models, such as finite element modeling (FEM), cellular automata, and machine learning techniques (Cui et al., 2022; Szeliga et al., 2022), to capture the complex, multi-scale behavior during hot rolling.

TABLE 2.8: Table showing the influence of hot rolling on microstructural evolution

Mechanism/Feature	Effect of Hot Rolling	Influencing Factors	Key References
Dynamic Recovery	Dislocation rearrangement and annihilation	Temperature, SFE	Liu & Lin (2003); Tayyebi & DerakhshaniMolayousefi (2023)
Dynamic Recrystallization	Grain refinement, strain-free grains	Strain, temperature, SFE	Wang et al. (2006); Liu & Lin (2003); Cui et al. (2022)
Grain Size Evolution	Grain refinement or growth	Rolling strain, temperature, alloy composition	Wang et al. (2006); Cui et al. (2022); Frazier et al. (2024)
Texture Development	Preferred orientations, elongated grains	Rolling direction, reinforcements, annealing	Ghazanlou et al. (2021); Han et al. (2023)
Heterogeneous Evolution	Localized DRX, property gradients, phase-induced variations	Reinforcements, rolling schedule, thermal profile	Szeliga et al. (2022); Frazier et al. (2024)

2.4.4 Influence of high temperature hot rolling on texture evolution

High temperature Hot rolling significantly influences the evolution of crystallographic texture in metals and alloys, affecting their mechanical and physical properties. The process parameters, alloy composition, and initial microstructure all play crucial roles in determining the final texture.

Mechanisms of Texture Evolution

Deformation and Slip Systems: Hot rolling activates specific slip systems, such as {111}<110> in Al-Cu-Mg alloys, leading to the development and rotation of textures like α-fiber and Brass components as deformation increases. Higher rolling temperatures enhance Brass texture intensity due to increased slip rates and lower substructural energy density in Brass subgrains.

Dynamic Recrystallization: In β-titanium alloys, dynamic recrystallization during hot rolling weakens deformation textures and introduces texture gradients through the thickness, as recrystallized grains rotate towards preferred slip systems.Recrystallized grains often inherit the orientation of the deformed matrix, especially when nucleation occurs at bulged boundaries

Influence of Rolling Parameters and Alloy Composition:

Reduction and Rolling Path: The degree of reduction and rolling path (e.g., unidirectional vs. cross rolling) strongly affect texture. Higher reductions can rotate textures (e.g., α-fiber to Brass in Al-Cu-Mg alloys) and alter surface vs. center layer textures.

Alloying Elements: Additions of elements like Zn and Ca in Mg alloys weaken basal textures by promoting pyramidal slip and reducing twinning activity, resulting in split basal textures and overall weaker texture intensity8. Rare earth additions can induce unique textures that evolve with increasing strain

Mechanical and Magnetic Anisotropy: Texture evolution during hot rolling directly impacts anisotropy in mechanical and magnetic properties. For example, certain hot band textures in Al alloys lead to distinct anisotropy profiles after further processing.while in electrical steels, optimal hot rolling reduction enhances beneficial recrystallization textures and magnetic induction.

In summary, hot rolling drives significant texture evolution through deformation mechanisms, recrystallization, and the interplay of process parameters and alloy composition. These changes are critical for tailoring the final properties of metals and alloys.

2.4.5 Effect of hot rolling on mechanical properties

High temperature Hot rolling significantly alters the mechanical properties of magnesium (Mg) alloys by refining their microstructure, changing phase distributions, and affecting strength and ductility. The main effects are increased strength and yield, grain refinement, and a optimum balance between strength and ductility depending on rolling temperature and post-processing.

1. Strengthening Effect of Hot Rolling

Hot rolling significantly enhances both yield strength (YS) and ultimate tensile strength (UTS) of Mg based alloys through grain refinement, strain hardening, and phase redistribution. According to Wang et al. (2010), hot rolling of Mg-5Al-0.3Mn-2Nd alloy resulted in an increase of YS from 77 MPa (as-cast) to 153 MPa and UTS from 180 MPa to 215 MPa. This improvement was primarily because of the finer grain structure and the uniform distribution of the second phases.

Similarly, Rogachev et al. (2024) demonstrated that hot rolling increased the YS of a Mg–Zn–Mn–Ca alloy from 106 MPa to 285 MPa (169% increase) and UTS from 210 MPa to 310 MPa (47.6% increase) when rolled at 300°C[42]. However, with increasing rolling temperature (400°C), the YS dropped to 200 MPa and UTS to 260 MPa, indicating a

trade-off between strength and ductility at elevated temperatures.

Li et al. (2024) also reported an exceptionally high UTS of 342 MPa in a hot-rolled Mg-5.5Gd-3Y-1Zn-0.5Mn alloy processed at 480°C with 60% reduction, demonstrating that rare earth and Zn additions significantly contribute to strengthening through solid solution strengthening and precipitation hardening mechanisms.

2. Ductility and the Strength–Ductility Trade-off

While hot rolling generally improves strength, it often results in reduced ductility due to strain hardening and elongated grain structures. For instance, Rogachev et al. (2024) found that elongation (El) dropped to 5% at 300°C but increased to 17% at 400°C, emphasizing the ductility recovery at higher temperatures due to enhanced dynamic recrystallization (DRX)[48]. This temperature dependence is also reported in Javaid and Czerwinski (2019), who observed elongation ranging from 17–21% in the ZEK100 alloy rolled at 350–450°C[43].

The optimum strength–ductility balance often requires careful temperature tuning. According to Xu et al. (2021), unconventional high temperature hot rolling of binary Mg alloys at tailored strain rates and temperatures helped enhance both strength and ductility by refining grains while preventing excessive work hardening.

3. Grain Refinement and Microstructure Evolution

Grain refinement is a primary strengthening mechanism during hot rolling, governed by dynamic recrystallization. The Hall–Petch relationship correlates smaller grain size with higher yield strength. Wang et al. (2010) observed a reduction in grain size from ~90 µm (as-cast) to ~20 µm after hot rolling, leading to the substantial increase in YS and UTS.

Javaid and Czerwinski (2019) similarly observed significant grain refinement in the ZEK100 alloy and noted that higher rolling temperatures improved DRX and homogenized the microstructure[43]. In another study, Ullmann et al. (2021) found that high temperature hot rolling of WZ73 (Mg-6.8Y-2.5Zn) alloy transformed coarse dendritic microstructures into a a refined equiaxed grain arrangement with evenly dispersed long-period stacking ordered (LPSO) phases.. These LPSO phases acted as DRX nucleation sites, refining grains and enhancing both strength and ductility.

4. Phase Transformation and Redistribution

Hot rolling modifies the morphology and distribution of precipitates in Mg based alloys, promoting uniformity and reducing brittleness. Wang et al. (2010) observed the breakup and more homogeneous distribution of second-phase particles (mainly Al11Nd3 and Mg17Al12) in hot-rolled samples, which reduced stress concentration zones and enhanced mechanical behavior.

Similarly, Li et al. (2024) noted that hot rolling dissolved large eutectic particles in Mg-5.5Gd-3Y-1Zn-0.5Mn alloy and replaced them with finer precipitates, contributing to both grain boundary pinning and precipitation strengthening.

5. Role of Dynamic Recrystallization (DRX)

DRX is a central mechanism during hot rolling of Mg alloys, especially at higher temperatures. It leads to the nucleation of new strain-free grains that replace elongated, deformed ones. Ullmann et al. (2021) found that DRX occurred predominantly at LPSO–α-Mg interfaces and triple junctions during hot rolling of WZ73 alloy.

Li et al. (2024) also confirmed that DRX occurred extensively in the hot-rolled Mg-Gd-Y-Zn-Mn alloy, especially at 480°C, resulting in ultrafine

grains and uniform texture. The dynamic recovery and recrystallization helped relieve internal stresses and improve mechanical isotropy.

6. Optimization via Rolling Temperature and Post-Processing

Achieving the optimal mechanical property profile requires fine-tuning of the rolling parameters and post-rolling treatments. **Javaid and Czerwinski (2019) recommend rolling at intermediate temperatures (~400°C) to strike a balance between strength and ductility[43].**

Rogachev et al. (2023, 2024) highlighted the importance of combining hot rolling with post-deformation annealing to restore ductility and reduce corrosion rates[42]. In their study, annealing of rolled Mg-Zn-Mn-Ca alloys led to a more equiaxed microstructure and improved elongation without severely compromising strength.

TABLE 2.9: Table showing the influence of high temperature hot rolling at different temperatures on mechanical properties like YS,UTS,percentage elongation.

Rolling Temp(°C)	Yield Strength (MPa)	UTS (MPa)	Elongation (%)	Reference
300	285	310	5	Rogachev et al., 2024
400	200	260	17	Rogachev et al., 2024
350–450	185–237	228–257	17–21	Javaid & Czerwinski, 2019
480(60% red.)	—	342	11	Li et al., 2024

2.4.6 Dynamic Recrystallization in Mg alloys

It is an important process during the hot deformation of magnesium (Mg) alloys, greatly influencing their microstructure and mechanical properties.

Types of DRX: Various DRX processes are identified in magnesium alloys, encompassing continuous dynamic recrystallization (CDRX), discontinuous dynamic recrystallization (DDRX), geometric dynamic recrystallization (GDRX), twin-induced DRX (TDRX), grain boundary bulging DRX (GBBDRX), and particle-stimulated nucleation (PSN), each contributing uniquely to microstructural refinement and mechanical behavior.

Mechanism Dependence: The dominant DRX mechanism depends on factors such as Zener-Hollomon parameter (Z), stored strain energy, grain size, and the presence of precipitates. For example, GDRX dominates at low Z, CDRX at intermediate Z, and DDRX at high Z.

Role of Twins and Particles: Twin-induced and particle-stimulated mechanisms can refine grains and promote DRX, especially in alloys with specific compositions or under certain deformation conditions.

Factors Influencing DRX:

Alloy Composition: Additions such as Bi, Gd, Y, and rare earth elements can refine grain size, accelerate DRX, and alter the dominant DRX mechanism.

Deformation Conditions: Temperature, strain rate, and strain level strongly affect DRX behavior. Higher temperatures and lower value of strain rates generally favor DRX, while specific mechanisms are activated depending on these parameters.

Microstructural Features: The presence and distribution of precipitates, grain boundaries, and twins influence nucleation and growth of recrystallized grains.

TABLE 2.10: Table showing the DRX Mechanisms in Mg alloys and factors influencing them

Mechanism	Key Influencing Factors	Typical Effects
CDRX	Moderate Z, low SSE, non-basal slip	Gradual grain rotation, refinement
DDRX	High Z, high SSE, grain boundary bulge	Nucleation at boundaries, rapid grain formation
GDRX	Low Z, geometric constraints	Grain subdivision, refinement
TDRX	Twin activity, coarse grains	Texture weakening, grain refinement
PSN	Large precipitates, high strain	Nucleation at particles

2.5 Heat Treatment via Annealing in Mg alloys

Heat treatment via annealing is a key process in tailoring the microstructure and mechanical properties of magnesium (Mg) alloys. Annealing can influence grain size, phase distribution, texture, and ultimately the strength, ductility, and resistance to corrosion of these alloys, making it crucial for optimizing their performance in various applications.

Microstructural Changes During Annealing

Grain Growth and Recrystallization: Annealing typically leads to grain growth and static recrystallization, increasing the proportion of fine equiaxed grains and reducing elongated grains. Higher annealing temperatures result in larger grain sizes, which can weaken certain textures and alter mechanical properties.

Phase Evolution: Annealing affects the dissolution and precipitation of secondary phases such as LPSO (long-period stacking ordered) phases, β-Mg17Al12, and other intermetallics. At higher temperatures, some phases

dissolve into the matrix, while others persist or coarsen, impacting the alloy's hardness and strength.

Texture Modification: Annealing can weaken strong fiber textures developed during extrusion or forging, leading to more random grain orientations and affecting mechanical anisotropy.

Effects on Mechanical Properties

Strength and Ductility: Annealing at moderate temperatures can increase ductility but often reduces strength and hardness because of grain growth and phase changes. At higher temperatures, both strength and ductility may decrease significantly.

Fracture Behavior: Annealing homogenizes the microstructure, enabling more stable crack propagation and increasing ductility, but reduces ultimate tensile strength and may eliminate certain fracture toughness characteristics.

Strengthening Mechanisms: Fine-grain strengthening is often more significant than solution or precipitation strengthening in annealed Mg alloys. Grain boundary strengthening dominates the yield strength, especially in alloys with rare earth elements.

Resistance to Corrosion and Other Properties

Corrosion Behavior: Increasing the volume fraction of certain phases (e.g., Mg17Al12) through annealing can improve corrosion resistance, as shown by lower corrosion current densities in treated samples. However, hardness may decrease with prolonged annealing.

Heat Capacity and Phase Transformations: Structural and phase transformations during annealing affect the heat capacity of Mg alloys, with specific phase transitions occurring in defined temperature ranges.

Optimization and Application

Tailoring Properties: By adjusting annealing temperature and duration, it is possible to balance strength and ductility for specific applications. Low-temperature annealing can maintain a favorable strength-ductility balance, while high-temperature annealing may degrade both.

Industrial Relevance: Optimized annealing schedules, such as T6 treatments, can produce high-performance, large-scale Mg alloy components suitable for industrial use.

2.5.1 Recrystallization and Texture Weakening via Annealing

Magnesium (Mg) alloys, despite their exceptional specific strength and lightweight nature, are limited in widespread structural applications due to poor formability and ductility. These deficiencies are primarily attributed to their strong basal texture developed during thermomechanical processing. Recent advances in thermomechanical processing and alloying strategies, particularly involving annealing treatments, have enabled significant improvements in formability by promoting recrystallization and weakening basal textures.

Mechanisms of Recrystallization and Texture Weakening

Twinning plays a vital role in the microstructural evolution during annealing. Double twins, in particular, serve as preferential nucleation sites for recrystallized grains. Guan et al. (2017) demonstrated that in a Mg alloy, annealing after deformation leads to nucleation at double twin intersections, contributing to random orientations and texture weakening. Their results revealed that twin-assisted recrystallization mechanisms could explain a substantial portion of texture evolution, with recrystallized grains showing a spread in orientation away from the basal plane. The SRX grains formed at twin and shear band intersections exhibited random orientations. **Their study found that the percentage of high-angle grain boundaries increased significantly during SRX, confirming grain boundary nucleation as a dominant mechanism**.

Roumina et al. (2022) :The real-time analysis revealed the dynamic nature of recrystallization front progression and grain rotation, validating the role of stored energy in grain boundary migration and texture weakening.

Nakata et al. (2022) proposed a novel cold-sample rolling method that induced a high density of double twins in a Mg-6Al-1Zn alloy. Upon annealing, these twins significantly contributed to the development of randomized textures, offering a promising route for achieving high ductility through texture engineering.

Influence of Alloying Elements: Alloying additions significantly alter recrystallization kinetics and texture evolution. Rare earth (RE) and transition metal additions such as Y, Gd, Ce, Ho, and Ca have been shown to modify recrystallization behavior profoundly. For instance, Peng et al. (2016) found that additions of Y, Ce, and Gd in Mg-Zn alloys led to delayed DRX and enhanced SRX, resulting in weaker basal textures and improved mechanical properties.

Kim et al. (2017) studied the Mg-Zn-Y system and reported that solute segregation at grain boundaries suppressed grain growth during SRX and promoted a more homogeneous microstructure. Their findings indicated that solute drag effects, along with particle-stimulated nucleation (PSN), played synergistic roles in texture modification.

Kumar et al. (2023) examined the Mg-10Ho alloy and observed that annealing promoted equiaxed recrystallized grains with high-angle grain boundaries[44]. This led to improved ductility (elongation > 30%) and reduced texture intensity. The basal texture intensity dropped below 4 m.r.d. (multiples of random distribution), confirming texture weakening.

Zhao et al. (2020) explored Zn and Ca content optimization in Mg alloys. They found that Zn increased SRX rates and Ca addition promoted transverse direction (TD) textures, thus reducing anisotropy. The Mg-2Zn-0.5Ca alloy showed a weakened basal texture and superior formability, with

an elongation of 30.1% and an Erichsen index of 6.7 mm.

Al and Zn additions also influence solute drag and recrystallization pathways. Jo et al. (2021) demonstrated that in non-flammable Mg-Al-Zn-Ca alloys, increasing Al content decreased basal texture intensity by broadening the orientation distribution. The highest Al-containing alloy showed a texture intensity of ~4 m.r.d., much weaker than traditional rolled Mg alloys.

Zhang et al. (2023) investigated Mg-Al-Ca alloys and found that anisotropic Ca segregation led to enhanced PSN and broadened basal poles. Their study showed that the intensity of basal texture dropped to 2.8 m.r.d. after isothermal annealing, indicating significant texture weakening.

Microstructure Evolution and Mechanical Properties

Annealing results in the evolution of microstructures from elongated, strain- hardened grains to equiaxed, recrystallized grains with more randomized orientations. This microstructural transformation enhances ductility and reduces anisotropy. Farzadfar et al. (2012) showed that grain sizes reduced significantly during SRX, resulting in finer microstructures and better elongation in Mg-2.9Y and Mg-2.9Zn alloys.

Kumar et al. (2023) found that hot-rolled and annealed Mg-10Ho alloys exhibited a refined grain size of ~8.3 μm, with improved yield strength (151 MPa) and elongation (34%)[44]. The mechanical improvements were because of mechanisms like solid solution strengthening, texture weakening, and grain boundary strengthening.

Jo et al. (2021) highlighted that with increasing Ca in solution and moderate Al content, texture broadening occurred.

Therefore,Recrystallization and texture weakening via annealing in Mg alloys are governed by a complex interplay of twinning, static recrystallization, and alloying strategies. Double twins and SRX serve as

effective nucleation sites for recrystallized grains with randomized orientations. Alloying elements like Y, Gd, Ce, Ho, Ca, Al, and Zn not only alter recrystallization pathways but also assist in weakening the basal texture and promoting non-basal orientations. By integrating tailored thermomechanical processing strategies and composition control, Mg alloys with superior ductility, formability, and mechanical strength can be achieved.

2.5.2 Recovery and Static Recrystallization Mechanisms

Recovery and static recrystallization are key processes that control the microstructure evolution and properties of magnesium (Mg) alloys during and after deformation. Understanding these mechanisms is essential for optimizing alloy performance, especially in applications requiring improved formability and mechanical strength.

Mechanisms of Recovery and Static Recrystallization

Recovery involves the rearrangement and annihilation of dislocations without the formation of new grains, reducing internal stresses. **In Mg alloys, static recovery (SRV) is observed in heat-affected zones and is often accompanied by continuous static recrystallization (CSRX) or discontinuous static recrystallization (DSRX), depending on cooling conditions and alloy composition.**

Static Recrystallization (SRX) is the formation and growth of new, strain-free grains during annealing after deformation. SRX can occur via continuous or discontinuous mechanisms, influenced by factors such as solute content, prior deformation, and the presence of twins or shear bands.

Influencing Factors

Alloy Composition: The presence of solute atoms like Mg, Zn, Ca, and Zr affects grain boundary mobility and recrystallization kinetics. Higher Mg content can initially slow down and later accelerate recrystallization due to

solute drag and fluctuation in dislocation density.

Deformation and Annealing Conditions: The amount and type of prior deformation (e.g., cold rolling, hot compression) and subsequent annealing temperature and time strongly influence recovery and recrystallization. High strain and low temperature favor dislocation accumulation, providing stored energy for SRX during later heat treatment.

Microstructural Features: Twins, shear bands, and grain boundary characteristics play significant roles. For example, {10-12} twins and dislocation structures can act as nucleation sites or barriers for recrystallization, affecting the rate and uniformity of new grain formation.

TABLE 2.11: Table showing different static recrystallisation mechanisms in Mg alloys and their influence on microstructure and texture evolution.

Mechanism	Conditions/Features	Observed Effects
Continuous SRX (CSRX)	Gradual subgrain rotation, high-angle boundaries	Uniform grain refinement, texture weakening
Discontinuous SRX (DSRX)	Nucleation and growth of new grains at boundaries	Heterogeneous grain size, localized texture change
Extended Recovery	Growth of recovered volumes within deformed grains	Texture evolution, mirror symmetry in basal poles

Microstructural Evolution and Texture

Recrystallization leads to significant changes in texture, often weakening the strong basal texture typical of Mg alloys and improving formability.

The dynamics of grain nucleation and growth during SRX are highly heterogeneous, with certain orientations showing preferential nucleation or growth advantages.

2.5.3 Influence of annealing on mechanical properties

Mechanisms and Microstructural Changes Induced by Annealing

Grain Refinement and Recrystallization: Annealing can promote static or dynamic recrystallization, leading to a refined, equiaxed grain structure and reduction of internal stresses. This generally results in improved ductility and formability. For instance, Yu et al. (2017) studied an as-extruded Mg- Gd-Y-Zn-Zr alloy and demonstrated that pre-annealing at 400°C facilitated dynamic recrystallization (DRX), significantly refining the grain structure[50]. Similarly, Yang et al. (2024) observed extensive recrystallization in Mg- Mn-Ce alloys annealed at 350℃ for 1 hour, which transformed elongated grains into fine equiaxed ones, thereby enhancing ductility.Cui et al. (2022) investigated Mg-3Y alloys and found that annealing at 300℃ refined the grain size from 17.6 μm to 6.8 μm, resulting in improved ductility and mechanical stability[49].

The strong basal texture typically formed during rolling or extrusion impairs ductility. Annealing weakens this texture and facilitates more random grain orientation. Yang et al. (2024) noted a significant basal texture weakening in Mg-Mn-Ce alloys after annealing at 350°C, contributing to reduced anisotropy. Song et al. (2024) reported a similar effect in Mg–Zn– Gd–Ca– Mn alloys, where the basal pole intensity decreased from 17.2 to 10.5 after annealing at 350°C for 1 hour[51].

Second Phase and Precipitate Behavior: Annealing also impacts the behavior of second-phase particles, including their dissolution, coarsening, or redistribution. For example, Sheng et al. (2020) analyzed Mg-Zn-Y-Nd alloys and observed that annealing at 350°C promoted the partial dissolution of secondary phases like Mg3Zn6Y and Mg12Nd, which delayed grain growth and preserved a fine-grained structure[52]. Kong et al. (2020) also demonstrated that subsequent annealing of caliber-rolled AZ31 Mg alloys caused coarsening of intermetallic phases, impacting both strength and ductility[53].

Effects on Mechanical Properties

Low to Moderate Annealing Temperatures: Low and moderate annealing temperatures (~250–300°C) are generally beneficial. They promote grain refinement and soften the material, improving ductility while maintaining adequate strength. For example, in the study by Zhang et al. (2021), Mg-6Al alloys processed via differential speed rolling and annealed at 300°C for 1 hour showed a balanced improvement: tensile strength remained at ~210 MPa, while elongation increased from 7% to 15%.Cui et al. (2022) reported that annealing at 300°C enhanced the elongation of Mg- 3Y alloys from 12.4% to 18.6%, with a slight reduction in yield strength from 228 MPa to 205 MPa[49]. This trade-off resulted in a significantly better strength-ductility synergy.

High Temperature and Long-Duration Annealing:At high temperatures (>350°C) or prolonged durations, significant grain coarsening and overgrowth of second phases are observed. This can degrade both strength and ductility. For instance, Sheng et al. (2020) found that annealing the Mg- Zn-Y-Nd alloy at 400°C for 1 hour caused grain coarsening from ~4.7 µm to ~15 µm and a reduction in ultimate tensile strength (UTS) from 296 MPa to 208 MPa[52].Kong et al. (2020) found that AZ31 Mg alloys annealed at 400°C showed a drop in yield strength from 198 MPa to 153 MPa, while ductility slightly declined due to excessive softening and grain growth[53].

Optimal Annealing Conditions:Optimal annealing conditions strike a balance between recrystallization, texture weakening, and control of grain growth. **Song et al. (2024) observed that annealing Mg–Zn–Gd– Ca–Mn alloys at 300°C for 1 hour resulted in a bimodal microstructure with fine DRXed grains and retained coarse grains[51]. This condition yielded a favorable combination of UTS (~284 MPa) and elongation (~19%). Zhang et al. (2021) emphasized that such bimodal structures promote work hardening while preserving ductility, making them perfect candidates for structural applications.**

Strength-Ductility Trade-Off and Alloy Tailoring: The inverse relationship between strength and ductility remains a fundamental challenge. **Annealing at progressively higher temperatures increases ductility but typically sacrifices strength due to grain coarsening and reduced dislocation density.** However, by fine-tuning the annealing schedule, a synergistic effect can be achieved.Yu et al. (2017) revealed that annealing Mg-Gd-Y-Zn-Zr alloys at 400°C for 1 hour increased elongation from 9.2% to 18.5% with only a moderate decrease in UTS from 321 MPa to 290 MPa[50]. This suggests that proper control of precipitate behavior and DRX can offset strength losses.Tailored annealing also improves corrosion resistance, as observed by Cui et al. (2022), where annealed Mg-3Y alloys exhibited improved surface passivation due to a refined grain structure and uniform second-phase distribution[49].

Chapter 3

RESEARCH GAP AND OBJECTIVE

Upon conducting an extensive literature survey on Mg alloys, particularly those alloyed with Bismuth (Bi) and processed through hot rolling followed by subsequent annealing, several critical research gaps were identified. These gaps highlight the need for gaining a more comprehensive insight into the progression of microstructure, the development of texture, and the associated mechanical properties. of Mg-Bi alloys under thermomechanical treatment. Based on these insights, the following research gaps have been outlined, followed by the specific objectives.

Research Gap

- The effect of hot rolling on the transformation of microstructure and the associated mechanical characteristics of magnesium-based systems when adding Bi as a solute element needs further investigation, since the study in this area is limited.
- There is a lack of systematic investigation into the relationship between grain size, dislocation density, texture evolution, and mechanical behavior in Mg-Bi alloys subjected to hot deformation.
- Limited data is available on how different annealing temperatures affect microstructural transformations such as recrystallisation, grain refinement, and activating the particular slip systems in Mg-Bi based alloys.

Research Objectives

- To examine the effect of high temperature hot rolling followed by further annealing at 225°C, 325°C, and 425°C on the microstructure evolution, texture evolution, mechanical behaviour, and deformation behavior of Mg-0.4wt% Bi alloy.
- To establish a clear correlation between annealing temperature and microstructural features like size of the grain, number of dislocations per unit volume and the activated slip systems that are present in the Mg-Bi alloy.
- To contribute to the understanding of how controlled thermomechanical processing can help optimize the strength-ductility balance in Mg-Bi systems.

Chapter 4

EXPERIMENTAL PROCEDURE

This section details the experimental approach, instrumentation, and procedural framework implemented to investigate the effects of elevated-temperature rolling followed by annealing on the behavior of Mg-0.4 wt% Bi alloys. It encompasses the protocols for specimen preparation, the specific thermal and mechanical processing conditions employed, as well as the analytical methods used to assess the microstructural evolution and mechanical response resulting from hot deformation and subsequent heat treatment.

4.1 Material & Proposed methodology

The Mg-Bi alloy utilizes magnesium as the base with bismuth enhancing its properties through Mg_3Bi_2 precipitate strengthening. Hot rolling and annealing lead to grain refinement and improved mechanical behavior. Its biodegradability makes it ideal for biomedical use, while its light weight and heat resistance suit automotive and aerospace needs. Enhanced corrosion resistance further expands its utility in protective coatings.

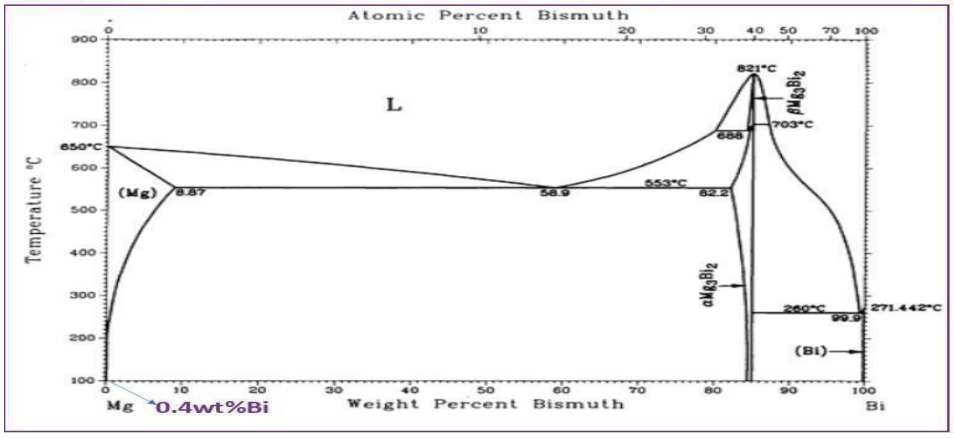

Fig 4.1:The phase diagram illustrating the interactions between magnesium and bismuth in the Mg–Bi binary alloy system.

The marked position on the Mg-Bi binary phase diagram in **Fig. 4.1** represents the specific composition of **0.4 wt% Bi** selected for alloying with magnesium in this study.

Proposed methodology:

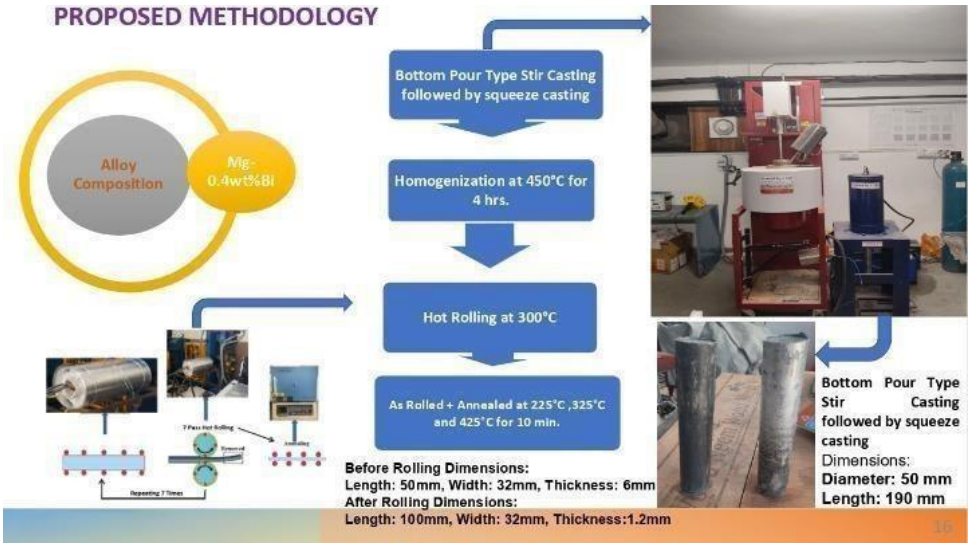

Fig 4.2:Shows the proposed methodology for the experiment

The outlined procedure depicted in Fig. 4.2 for fabricating the Mg-0.4 wt % Bi alloy starts with **bottom-pour stir casting**, followed by **squeeze casting** to produce an ingot measuring 50 mm in diameter and 190 mm in length. This cast ingot is then **homogenized at 450°C** for a duration of 4 hours. After homogenization, the material undergoes a **hot rolling process at 300°C, involving seven passes,** which alters the sample dimensions from an initial 50 mm length, 32 mm width, and 6 mm thickness to final dimensions of 100 mm length, 32 mm width, and 1.2 mm thickness. Finally, the rolled alloy is **annealed at temperatures of 225°C, 325°C, and 425°C, each for 10 minutes.**

4.2 Bottom poured Stir casting

In this process, the molten metal is introduced into the mold from the furnace's bottom while being vigorously stirred throughout the process.This method ensures uniform distribution of reinforcement

particles or alloying elements throughout the matrix, leading to a homogeneous microstructure with improved mechanical properties. The bottom-pouring mechanism reduces turbulence, minimizing defects like porosity and segregation, making it ideal for metal matrix composites and alloys requiring enhanced strength and stability.

Principle: Bottom-poured stir casting operates by pouring molten metal from the bottom of the furnace into a mold while continuously stirring the mixture. The bottom-pour mechanism minimizes turbulence, reducing defects like porosity and ensuring uniform distribution of reinforcement particles or alloying elements throughout the matrix. The stirring action enhances homogeneity, while controlled pouring improves particle dispersion, leading to a well-structured and mechanically stable composite or alloy.

Fig 4.3:Depicts the equipment used for bottom-poured stir casting.

Fundamental operating mechanism:

The fundamental mechanism includes the following stages:

Preheating Reinforcements – Reinforcement particles (e.g., SiC, Al_2O_3) are preheated to remove moisture and improve wettability with molten metal.

Melting the Matrix Alloy – The base metal (e.g., magnesium or aluminum) is heated in a furnace until it reaches the desired molten state.

Starting the stirring process – A mechanical agitator generates a vortex within the molten metal to promote thorough and consistent mixing.

Introducing Reinforcements – Preheated reinforcement particles are gradually added into the vortex to achieve homogeneous dispersion.

Degassing and Fluxing (Optional) – Inert gases or fluxes may be introduced to remove impurities and prevent oxidation.

Bottom Pouring into Mold – The molten composite is then introduced into a mold which is preheated through the furnace's bottom, reducing turbulence and promoting even dispersion.

Solidification and Cooling – The cast material is allowed to cool naturally or under controlled conditions.

Post-Processing – The solidified casting undergoes machining followed by further heat treatment or surface finishing as required.

This method enhances particle distribution, reduces defects.

4.3 Overview of the Squeeze Casting process

This method integrates the beneficial aspects of both casting as well as forging. Here,the molten metal is poured into a mold cavity and subjected to high compressive pressure, which is maintained throughout the solidification phase. This technique leads to the fabrication of parts with superior mechanical integrity and significantly reduced internal defects when compared to traditional casting approaches.

The fundamental steps involved in its process are outlined below:

1. Mold preparation: To ensure the metal solidifies efficiently, the die is initially brought to a carefully controlled high temperature before the casting process begins. Typically, it is made from durable materials like hardened steel to withstand the high pressures exerted during the process.

2. Molten Metal Transfer: The molten metal—often lightweight alloys such as magnesium or aluminum—is poured into an intermediate reservoir (like a gooseneck or sleeve), which regulates and controls the flow into the mold cavity.

3. Pressure Application: A ram or hydraulic actuator applies continuous force on the molten metal in the chamber, driving it steadily into the die. This pressure is maintained throughout the entire solidification process.

4. Solidification under Pressure: With the pressure held constant, the metal begins to crystallize, leading to a refined grain structure that enhances strength, reduces internal porosity, and improves overall density consistency.

5. Part Extraction: Once the material has fully solidified, the applied pressure is released, and the finished component is carefully removed from the mold.

Key terms frequently linked to the squeeze casting process include:

1 Applied Squeeze Pressure: The force exerted on the molten metal during its transition to solid form, which is essential for enhancing the casting's compactness and mechanical strength.

2. Shot Sleeve: A containment chamber linked to the mold, designed to regulate the precise flow of molten metal as it is injected into the pre-formed mold.

3. Die: The molten metal is directed under pressure into a pre-formed mold specifically shaped to define the final geometry of the cast component.; usually fabricated from tough materials like steel to endure the significant pressures present in squeeze casting.

4. Porosity: The occurrence of tiny cavities or trapped air within the cast structure; squeeze casting significantly minimizes these imperfections compared to traditional casting techniques.

Equipments utilized in the squeeze casting technique includes:

1. High-Pressure Squeeze Casting Machine: A dedicated apparatus engineered to exert substantial force on molten alloys during solidification. It incorporates components such as a shot sleeve, a plunger or piston, and a pressure-generating system—either hydraulic or mechanical—to regulate and maintain force throughout the process.

2. Temperature Monitoring equipments: Accurate thermal regulation is vital in squeeze casting to achieve uniform solidification and reduce formation of flaws. This is accomplished using systems like gas or electric heaters, which precondition the die and sustain target temperatures during the entire operation.

3. Pressure Monitoring equipments: Devices including gauges and pressure sensors are integrated into the setup to oversee the force exerted on the molten metal. These tools ensure that the pressure remains consistent and within the desired range for the necessary duration.

4. Mold Release Mechanisms: Once solidification is complete, mechanisms such as ejector pins or hydraulic actuators are employed to

assist in removing the casting from the die efficiently, avoiding deformation or damage to the finished part.

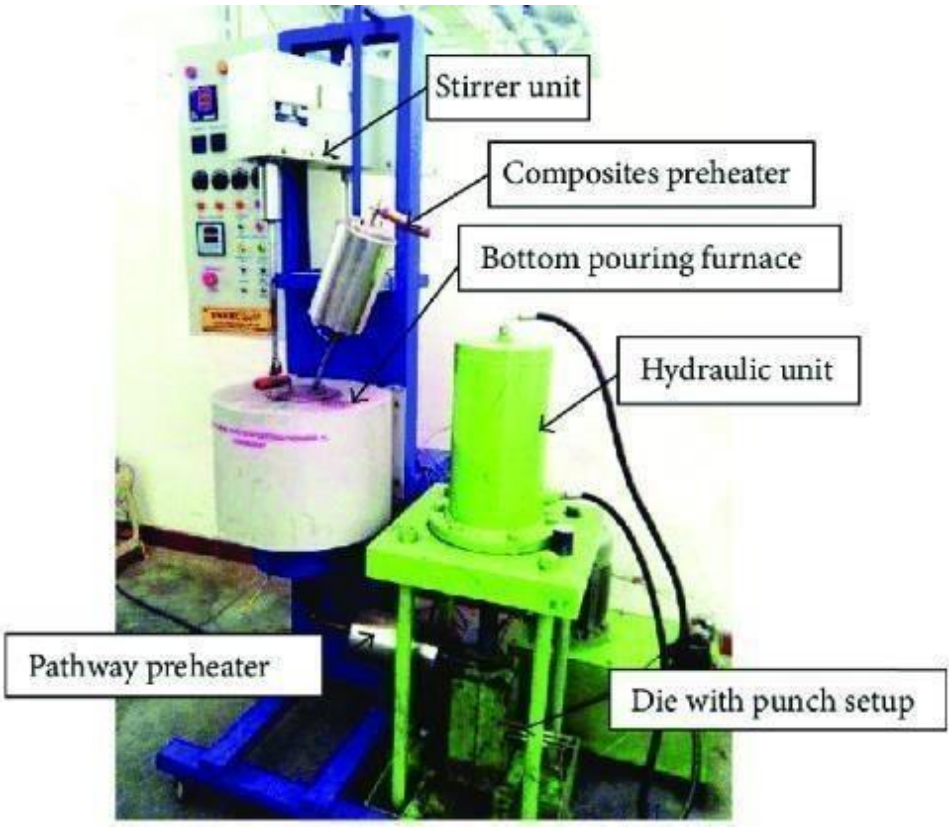

Fig 4.4::Depicts the equipment utilized for the squeeze casting process.

4.4 Overview of the Homogenization process

Homogenization in magnesium refers to a thermal treatment method designed to promote microstructural uniformity throughout the material. This process involves elevating the temperature of magnesium to approximately 693 K—just below its melting threshold—followed by a controlled cooling phase. The applied heat encourages the redistribution of solute-enriched zones or segregated phases, ultimately resulting in a more homogeneous internal structure and improving the alloy's formability during subsequent processing steps.

Homogenization represents a diffusion-driven annealing technique, wherein a metal or alloy is subjected to elevated temperatures for a defined period followed by a cooling cycle that"s slow. This is primarily employed to improve the ease of machining and also to alleviate internal stresses that might otherwise lead to distortion or fracture. However, pure magnesium exhibits limited responsiveness to this process. As a result, homogenization is effectively applied only to magnesium alloys that incorporate elements such as copper, zinc, or alloying systems like aluminium-silicon. A comparable approach is necessary for other metals, including manganese and aluminium, which also depend on the presence of specific alloying constituents for homogenization to yield beneficial outcomes.

4. 4. 1 The overview of the execution of the Homogenization Process

Having understood the fundamentals of the magnesium homogenization process, we now turn our focus toward exploring its detailed operational parameters.

4. 4. 1. 1 Overview of the execution of Heating Process

In magnesium alloy systems, the thermal parameters required for effective homogenization are carefully maintained just beneath the alloy's melting point. Although the exact temperature varies based on the specific alloying elements involved, it typically remains under 900°C. For most compositions, the process is conducted around 693 K. Surpassing this critical thermal window can result in oxidation or structural deformation, thereby compromising the integrity of the material. Additionally, the time over which heat is applied—generally spanning 4 to 5 hours—is tailored to the part's thickness, ensuring thorough diffusion throughout its volume.

4. 4. 1. 2 Overview of the execution of Cooling Process

Once the heating stage is finalized, the alloy is subjected to a controlled cooling routine. This process often starts with quenching in a suitable

medium, followed by a slower temperature decline. The cooling pace is tailored according to the alloy's unique elemental makeup. It is critical to move magnesium-based alloys directly from the furnace into the quenching environment to preserve the thermal-induced geometry. During their initial solidification, magnesium and the added alloying elements are often distributed unevenly. The homogenization treatment promotes a more uniform atomic arrangement, which is gradually locked in as the material cools post-treatment.

4. 4. 2 Advantages of Performing Homogenization on Magnesium

In contrast to other thermal treatment techniques, homogenization does not contribute to increasing a material's mechanical strength or fracture resistance. Its primary advantage lies in enhancing the material's formability and in minimizing structural inconsistencies or imperfections.

4 .4 .2. 1 Produce a material that is easier to shape and process.

A primary aim of homogenising a material is to enhance how easily a material can be machined. Magnesium that has undergone homogenization demonstrates improved ductility and machinability, making it a far more effective candidate for the fabrication of precision-engineered parts.

4 .4. 2. 2 Develop a material with enhanced compositional consistency throughout.

In the fabrication of magnesium-based alloys, the distribution of alloying constituents tends to be non-uniform, resulting in localized discrepancies in mechanical responses such as hardness and elasticity—factors that compromise the material's suitability for precision machining. The process of homogenization mitigates this issue by promoting a more even spatial redistribution of the elemental additions within the matrix, ultimately yielding a structurally consistent alloy with reliable mechanical behavior throughout.

4. 4. 2. 3 Enable Compatibility with Subsequent Thermal Processing

Following the completion of the homogenization cycle, magnesium becomes well-prepared for subsequent heat-based treatments such as solution heat treatment. Additionally, it may be processed through cold working—where mechanical force is applied at ambient temperatures—to refine its strength characteristics without the influence of elevated thermal input.

4. 5 EDM process

This process represents an unconventional fabrication technique wherein material removal is achieved through a series of rapid electrical discharges that erode the metal surface. This approach proves highly effective for crafting complex profiles and is particularly advantageous when dealing with materials that are otherwise challenging to machine. In the context of our study, the Wire EDM configuration was utilized. The subsequent sections delve into the working principles, defining terminology, and primary components integral to this process.

Fundamental Operating Mechanism of EDM:

1. Initial Setup Phase: In this phase, the material to be shaped and a specially designed electrode—typically made of copper or graphite due to their high electrical conductivity—are completely submerged in a dielectric fluid, most often deionized water. The electrical setup ensures that the workpiece acts as the anode, being connected to the positive terminal of the power source, while the electrode serves as the cathode, attached to the negative terminal. This arrangement facilitates the controlled removal of material through a series of electrical discharges, allowing for precise shaping of the component.

2. Initiation of Electrical Discharge: A controlled electrical spark is

generated between the electrode and the workpiece, concentrating thermal energy at targeted spots. This intense heat causes small areas of the material to melt and vaporize, creating microscopic craters on the surface.

3. Material Removal Process: The molten and vaporized debris is swiftly flushed away by the circulating dielectric fluid, which also helps maintain an optimal gap between the electrode and the workpiece. These high-frequency pulsed discharges progressively erode the material, shaping it to mirror the electrode's form.

4. Control of Accuracy and Surface Finish: Key parameters—including energy per discharge, pulse duration, pulse frequency, and electrode movement—are precisely regulated for getting dimensions and surface quality as needed of the finished component.

Key Terms and Definitions related to EDM process:

1. **Dielectric insulating Fluid:** This is an electrically non-conductive liquid, most commonly deionized water, that facilitates spark generation, removes debris from the machining zone, cools the workpiece surface, and prevents unintended electrical arcing between the electrode and the workpiece.

2. **Graphite Electrode:** A carefully crafted tool fabricated using graphite, serving as the negative terminal (cathode), which gradually erodes material from the surface of the metal workpiece.

3. **Metal Workpiece:** The conductive metal or alloy component that is subjected to the machining process.

4. **Electrode-to-Workpiece Gap:** The very small clearance, typically on the order of tens to hundreds of microns, between the electrode and workpiece where the electric discharge sparks occur.

5. **Dielectric Fluid Flushing:** A continuous flow of fresh dielectric liquid directed at the machining interface to remove molten debris and maintain

a contaminant-free gap for stable spark generation.

Key Components of The EDM Machine:

1. Power Power Supply Unit: This equipment provides the essential high-frequency electrical pulses needed for the EDM operation. It precisely controls factors such as voltage, current intensity, and pulse duration to ensure accurate and controlled material removal.

2. EDM CNC (Computer Numerical Control) System: Modern EDM machines utilize a computer-driven control system that governs the electrode's trajectory. It interprets CAD/CAM data and converts it into exact instructions to steer the machining process effectively.

3. Primary EDM Machine: This apparatus performs the electrical discharge machining and consists of several components, including the power supply, CNC controller, worktable, electrode holder, dielectric fluid circulation mechanism, and other vital parts necessary for efficient machining.

4. Gap Monitoring Devices: Specialized sensors and monitoring tools are employed to continuously observe the spark gap, tracking parameters such as discharge intensity, inter-electrode spacing, and stability of the electrical spark during the machining cycle.

5. Filtration Equipment: During the EDM process, the dielectric fluid becomes contaminated with eroded particles. A filtration system is used to purify the fluid by removing debris, thereby preserving fluid quality and maintaining machining performance.

Fig 4.5::Displays the Wire EDM(electric discharge machining)machine

4. 6 Thermal Processing Applied to Magnesium-Based Alloys

Heat treatment is widely employed to augment the mechanical performance. By carefully applying controlled heating and cooling cycles, the alloy's internal microstructure is altered, leading to improvements in strength, ductility, and other beneficial properties. Below are several prevalent heat treatment methods utilized specifically for magnesium alloys:

Solution Solution Heat Treatment: This process involves heating the magnesium alloy to elevated temperatures, enabling the soluble phases to dissolve into the magnesium matrix. This promotes a chemically homogeneous structure, reducing microscopic inconsistencies. The temperature and soaking duration are precisely controlled according to the alloy's composition and the desired mechanical enhancements targeted by this treatment.

Quenching: Quenching refers to the rapid cooling of the alloy from the solutionizing temperature down to ambient temperature. The aim is to trap

the microstructure in a supersaturated solid solution, beyond equilibrium solubility, which leads to improved mechanical characteristics like greater ductility and strength. Different quenching media—such as air, water, or oil—are chosen based on the alloy type and the intended properties.

Aging: Conducted after solution treatment and quenching, aging involves holding the alloy at an intermediate temperature for a specified time to allow precipitation or phase changes. This step significantly raises hardness and mechanical strength by encouraging the formation of precipitates or secondary phases within the microstructure. Precise control of temperature and time during aging is essential to balance strength and ductility effectively.

Annealing: This involves heating the magnesium alloy to a temperature below its melting point and maintaining it for a predetermined period, followed by slow cooling. This heat treatment aims to relieve residual stresses, increase ductility, and refine the microstructure.

Recrystallization: Recrystallization is applied to magnesium alloys to produce a finer, more uniform grain structure. The alloy is heated to a temperature where new, strain-free grains nucleate, replacing the deformed grain structure caused by prior mechanical work. This process enhances mechanical properties such as ductility and formability by reducing grain size and improving grain boundary characteristics.

4. 7 High temperature Hot Rolling

Hot rolling at elevated temperatures entails deforming metal by first raising its temperature above the recrystallization point, followed by passing it through a series of rolling mills. This operation diminishes the metal's thickness while shaping it into the desired cross-sectional profile. Below is an outline of the core concepts and procedural specifics related to the hot rolling method:

Overview of the working principle of high temperature hot rolling:

The core principle of hot rolling centers on applying intense compressive pressure to a heated metal billet or slab, which results in plastic deformation and a reduction in thickness. Heating the metal increases its softness and ductility, facilitating easier shaping into the required form.

Fundamental Operating Mechanism of high temperature hot rolling:

The hot rolling process at elevated temperatures typically follows these stages:

1. Metal Heating: Inside the furnace, the metal is thermally treated until it attains its recrystallization threshold. The exact thermal input is tailored according to both the specific category of the metal and the intended set of mechanical characteristics to be achieved.

2. Introducing Metal to Rollers: After reaching the desired thermal condition, the metal is directed into the rolling mill, where it undergoes deformation by sequentially passing through multiple rollers. These rollers exert compressive forces that sculpt the metal in alignment with predefined dimensional requirements.

3. Thickness reduction: While progressing through the roller assembly, the metal is subjected to compressive stress, leading to a progressive reduction in its cross-sectional thickness. Depending on the requirements, the rollers can have smooth or textured surfaces to impart specific profiles or finishes.

4. Cooling of Rolled Metal: After shaping, the metal undergoes cooling — often through water sprays or other cooling techniques—to prevent overheating and maintain the mechanical qualities obtained during rolling.

5. Cutting and Finishing: The final step involves cutting the rolled metal into

desired lengths and preparing it for packaging or further manufacturing processes.

Fig 4.6::Depicts the high temperature Hot Rolling equipment.

4.8. Analysis of Mechanical Behavior and Characterization

4.8.1. Overview of the Universal Testing Machine (UTM)

This machine functions as an all-encompassing mechanical testing apparatus designed to evaluate critical material characteristics including tensile strength, compressive strength, shear capacity, and hardness. This versatile instrument performs various mechanical tests by exerting different types of loads.The fundamental concept behind a Universal Testing Machine (UTM) is to exert a precisely regulated force on the specimen while simultaneously recording the amount of deformation it undergoes. This dual measurement enables precise determination of the material's response to diverse stress conditions.

4.8.1.1 Key Components

Key components such as the load frame, crosshead, load cell, displacement sensor, and a user control interface. The load frame serves as the main structural support, ensuring stability and proper alignment of the specimen during testing. The crosshead, connected to the load cell, moves vertically according to the system's instructions. The load cell measures

and records the force applied to the test sample, while the displacement sensor monitors the amount of deformation the specimen undergoes throughout the test. Through the control interface, operators can set crucial testing parameters like the force magnitude and crosshead speed, while also observing real-time data to track the progress of the experiment.

4.8.1.2 Fundamental Operating mechanism

The fundamental operation of a Universal Testing Machine (UTM) hinges on the interplay between stress and strain.When a load is exerted, the corresponding stress is determined by taking the force magnitude and dividing it by the specimen's initial cross-sectional area. This induced stress leads to deformation, which is precisely tracked using a displacement sensor.

The UTM's flexibility allows it to perform various testing procedures by imposing different types of loads. For instance, during a bending test, a force is applied centrally to a beam or rod, and the degree of bending or deflection is recorded to evaluate the material's flexural strength.

In essence, the Universal Testing Machine is an essential device for assessing the mechanical properties of materials, capable of delivering regulated forces while accurately measuring the deformation response. Its key components include the load frame, crosshead, load cell, displacement measurement device, and a user interface for controlling and monitoring the test.

4.8.2 Microscopical Analysis

Microscopical analysis refers to the thorough investigation of samples using microscopes—devices engineered to enlarge and enhance the visibility of minute details that are invisible to the naked eye. This method is a crucial analytical approach employed extensively in various scientific

and engineering disciplines such as materials science, nanotechnology, chemistry, and biological studies. By uncovering complex structures at micro and nanoscale levels, microscopical analysis plays a vital role in driving progress and innovation within both research and industrial applications.

4.8.2.1 Optical Microscopy analysis

This is a technique that employs visible light along with a system of lenses to magnify and examine the fine structural details of a specimen.

The core principle behind an optical microscope involves illuminating the specimen with a visible light source—commonly provided by LEDs or incandescent lamps—and using a series of lenses to magnify the resulting image.This light is first gathered and magnified by the objective lens positioned close to the sample. The enlarged image produced is then transmitted to the eyepiece lens, which further magnifies it so that the observer can view the intricate details of the specimen.

Optical microscopes come in various designs, each optimized for specific imaging requirements. These variations include brightfield microscopes, phase contrast types, and fluorescence microscopes, each offering unique imaging capabilities and contrast techniques tailored to different sample characteristics.

A conventional optical microscope consists of several key components: a light source, an objective lens assembly, an eyepiece, and a movable stage that holds and allows precise positioning of the specimen. The illumination system—which may range from simple incandescent bulbs or LEDs to advanced lighting modules—provides steady and adjustable lighting to improve image quality. The objective lens, situated nearest to the sample, is responsible for collecting the light that interacts with the

specimen and delivering the initial magnification of its features. This magnified image is then enhanced further by the eyepiece, giving the user a clear and detailed view. The specimen stage secures the slide and often includes fine-tuning controls to adjust the sample's position vertically and horizontally, aiding in focusing.

Modern optical microscopes often incorporate advanced features such as motorized stages for automated sample scanning, integrated digital cameras for capturing high-resolution images, and sophisticated software for detailed image analysis and quantitative measurements, greatly expanding their functionality beyond traditional setups.

4.8.2.2 Scanning Electron Microscopy (SEM) analysis

Its an advanced analytical method used to reveal information about surface features and elemental makeup of materials. This approach works by directing a precisely focused electron beam to scan the specimen's surface systematically in a raster fashion. When these electrons interact with the material's surface, a range of signals—including SE and BSE electrons are emitted and collected, enabling the generation of highly detailed images alongside compositional insights.

The core principle of SEM revolves around analyzing these emitted signals, which reveal surface morphology, texture, and elemental distribution of the sample. In comparison to conventional optical microscopy, SEM offers enhanced image clarity and contrast, establishing it as a vital instrument in disciplines such as materials science, metallurgy, and nanotechnology.

An SEM system typically comprises several crucial components: an electron gun that produces the primary electron beam, electromagnetic lenses that focus the beam precisely, scanning coils that steer the beam

across the specimen, a vacuum chamber designed to prevent electron scattering by air molecules, detectors for capturing the emitted signals, and a computer interface responsible for data processing and visualization. Together, these elements allow for real-time, high-resolution exploration of microstructural details across a wide variety of samples.

Fundamental operating mechanism of SEM :

1. Electron Beam Production: The electron gun generates a tightly focused stream of electrons, which are then accelerated and accurately guided onto the specimen through the use of electromagnetic lenses.

2.Interaction of Electron Beam with the Specimen: Upon striking the specimen's surface, this concentrated electron beam triggers the emission of various signals, including:

i) Emission of Secondary Electrons (SE) Emission: These are low-energy electrons ejected from the surface atoms due to the impact of the primary beam, offering high-resolution details of the specimen's surface morphology and texture.

ii) Emission of Backscattered Electrons (BSE): These higher-energy electrons are reflected after interacting with the atomic nuclei within the sample, producing contrast in the image that corresponds to variations in elemental composition, as their behavior is influenced by differences in atomic number.

iii) Emission of X-Rays : The collision of the primary electron beam with the atoms of the specimen can also generate characteristic X-rays, which are utilized to determine the elemental makeup of the material.

3. Signal Acquisition using Detectors: Situated above the specimen, an array of specialized detectors collects these emitted signals. Different

detectors are optimized for capturing specific emissions—for instance, secondary electron detectors focus on SE signals, while solid-state detectors are employed to detect both backscattered electrons and characteristic X-rays.

4. Final Image Generation: The collected signals undergo amplification and electronic processing, transforming them into electrical signals that create a visual representation on a monitor.

Key Terms and Definitions related to SEM analysis :

1. Sample or Specimen: This refers to the material being analyzed within the Scanning Electron Microscope. It may exist in various forms—such as bulk solids, powdered substances, or thin layers that are often coated with a conductive film to enhance image clarity during observation.

2. Electron Gun: Acting as the electron emitter, the electron gun generates a stream of electrons through thermionic emission from a heated filament. This beam is then directed and refined using a series of electromagnetic lenses for precise targeting onto the sample surface.

3. Electron Optics System: This assembly includes the electromagnetic focusing elements and apertures responsible for controlling the path and intensity of the electron beam. It ensures proper acceleration, alignment, and convergence of the beam onto the designated point on the specimen.

4. Scanning electromagnetic Coils: These are electromagnetic devices that systematically deflect and sweep the electron beam across the sample surface in a raster format. This scanning motion allows the microscope to gather spatially resolved information from the entire scanned area.

5. High-Vacuum Environment: A critical part of SEM functionality, the vacuum system maintains low-pressure conditions within the chamber.

This vacuum reduces interactions between the electron beam and air molecules, preserving beam quality and ensuring accurate signal detection from the sample.

Components of Scanning Electron Microscope (SEM) Machine:

1. **Electron Column:** This vertical structure comprises all essential components that generate and manage the electron beam, including the electron gun, focusing lenses, and beam-limiting apertures. Together, they direct and shape the beam with high precision before it reaches the specimen.

2. **Signal Detectors:** A variety of detectors are integrated to capture distinct types of emissions from the specimen. The Everhart-Thornley detector is typically used for acquiring secondary electron data, which is valuable for surface morphology. In contrast, solid-state detectors are utilized to register backscattered electrons and characteristic X-ray emissions for compositional insights.

3. **Image Display System:** After signal acquisition, this subsystem processes the data through amplification and electronic conversion. The processed signals are then visualized using imaging software that reconstructs the topographical or compositional information into a coherent digital image on the display interface.

4. **Specimen Stage:** This is the adjustable mount where the sample is secured. It allows for fine movements, including rotation, tilt, and translation, to facilitate examination of various areas and orientations of the specimen for comprehensive surface analysis.

5. **Vacuum Maintenance System:** This setup sustains the low-pressure conditions essential for SEM operation. Composed of vacuum pumps,

valves, and pressure-monitoring instruments, it eliminates atmospheric interference, enabling unimpeded electron travel from the source to the sample.

4.8.2.3 Electron Backscatter Diffraction (EBSD) analysis

It is used within an electron microscope to study the crystallographic attributes of materials. This technique facilitates detailed mapping of features such as grain orientation, grain boundary networks, and the presence of crystallographic imperfections. It enables researchers to visualize and quantify the internal structure of crystalline solids at a fine scale. Below is a breakdown of the fundamental operating mechanism, relevant key terms and terminology, and the instrumental components involved in EBSD analysis:

Fundamental Operating mechanism of EBSD analysis :

1. Interaction Between Electron Beam and Sample: In an electron microscope, a focused beam of electrons is projected onto the surface of a crystalline sample. Upon contact, a portion of these electrons is reflected back, and some undergo diffraction due to the atomic arrangement in the crystal lattice.

2. Formation of Kikuchi Patterns: The diffracted backscattered electrons interfere with one another—constructively and destructively—creating a distinct pattern known as a Kikuchi or electron backscatter diffraction pattern. These patterns encode carry embedded details regarding the spatial orientation and arrangement of the crystal planes.

3. Detection of the Diffraction Pattern: This characteristic diffraction pattern is registered using a dedicated EBSD detector, typically situated above or at an angle to the sample. The resulting image displays bands or

lines corresponding to the crystallographic structure.

4. Crystallographic Data Extraction: Advanced computational techniques are used to decode the captured pattern. These algorithms interpret the orientation of the crystal lattice, identify grain boundaries, and reveal various features of the crystal structure based on the symmetry and geometry of the diffraction lines.

Key Terms and Definitions related to EBSD analysis :

1. Crystal Orientation: Refers to the spatial alignment and directional arrangement of atomic planes within a crystalline material. This orientation is characterized with respect to the crystallographic coordinate system specific to each crystal structure.

2. Grain: Denotes a distinct zone within a polycrystalline material where the atomic lattice maintains a uniform directional configuration. These regions are separated by interfaces known as grain boundaries.

3. Grain Boundary: Acts as the transitional region or interface between two neighboring grains that possess differing orientations of their internal crystal lattices. These boundaries vary in nature, ranging from slight misalignments (low-angle boundaries) to significantly differing orientations (high-angle boundaries).

4. Kikuchi Pattern: Commonly referred to as the electron backscatter diffraction pattern, this unique band pattern emerges as a result of electron diffraction, which occurs when incident electrons interact with the crystal's regularly repeating atomic lattice. Analysis of these patterns provides insight into the crystallographic features of the sample.

Components of EBSD Machine:

1. Electron Microscope: Scanning electron microscope (SEM) or transmission electron microscope (TEM) serve as the foundational platform for EBSD by producing a focused beam of electrons and enabling the observation of the sample under investigation.

2. Electron Backscatter Diffraction Detector: This dedicated detection unit, placed strategically above the specimen inside the microscope chamber, is responsible for gathering and recording the diffraction patterns generated by backscattered electrons interacting with the crystal structure.

3. Phosphor Screen: A key component within the detector, the phosphor screen functions by transforming the incoming diffracted electrons into a visible light pattern, facilitating real-time visualization of the diffraction image.

4. Charge coupled device Camera: Modern Electron Backscatter Diffraction (EBSD) systems utilize a Charge-Coupled Device (CCD) camera to record the illumination emitted by the phosphor screen. This optical data is then transformed by the camera into a digital representation, enabling subsequent computational analysis.

5. EBSD Software: Dedicated analytical software processes the digitized diffraction data. Using sophisticated pattern recognition algorithms, indexing methods, and crystallographic matching tools, the software extracts precise information about orientation, boundary characteristics, and other structural features.

6. Stage Manipulator: A computer-controlled specimen stage allows for accurate adjustments in position, tilt, and rotation, enabling the systematic collection of diffraction data from various zones on the sample's surface.

7. Sample Preparation Equipment: Prior to EBSD examination, the specimen must be meticulously prepared using techniques like sectioning, mechanical grinding, fine polishing, and sometimes chemical or electrochemical etching. These steps are crucial for achieving a smooth, clean, and damage-free surface, which is essential for generating clear and interpretable diffraction patterns.

Chapter 5

RESULTS AND DISCUSSION

This section presents an in-depth analysis of the effects of hot rolling followed by subsequent annealing on Mg–0.4 wt% Bi alloys, focusing on microstructural evolution, texture modification, and mechanical performance. Through systematic investigation, we examine how thermomechanical processing influences grain refinement,texture,dislocation density,misorientation angle distribution,slip system activation,mechanical properties ultimately shaping the alloy's strength and ductility. The findings contribute to understanding the processing–structure–property relationship in Mg–Bi systems, providing insights into optimizing lightweight alloys for advanced structural applications.

5.1 SEM Micrographs for microstructural examination

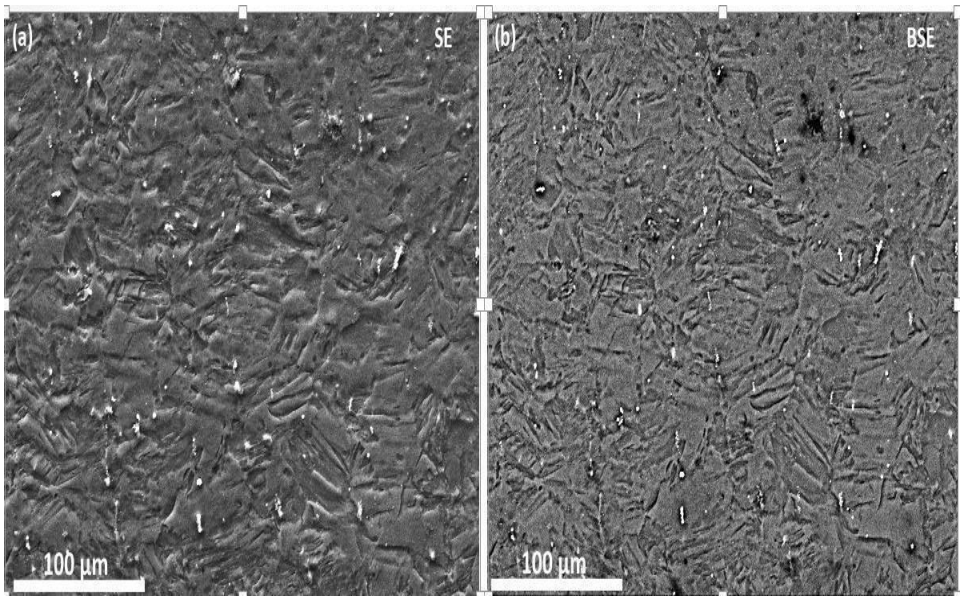

Fig. 5.1: SEM micrograph of Mg-0.4wt%Bi alloy where, (a) Secondary electron (SE) and (b) Back scattered electron (BSE) micrograph of alloy rolled at 300˚C .

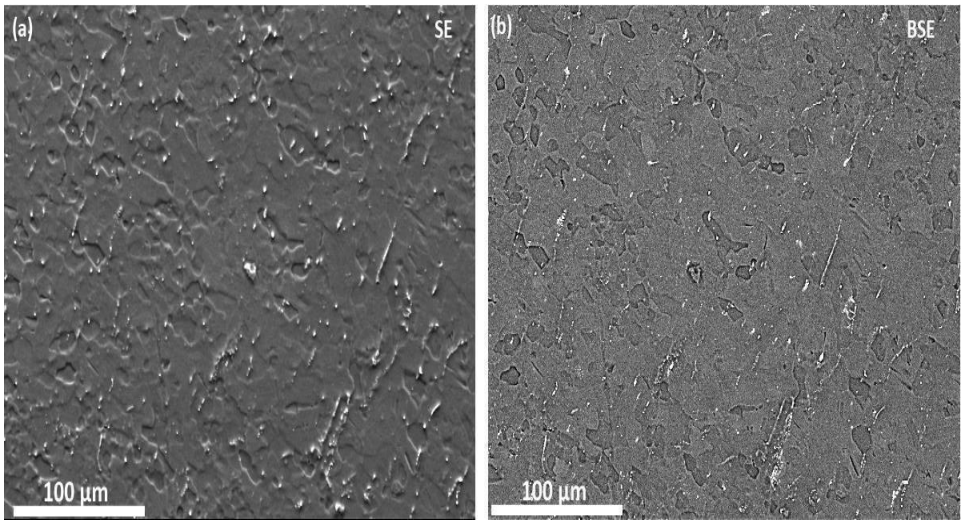

Fig. 5.2: SEM micrograph image of Mg-0.4wt%Bi alloy where, (a) Secondary electron (SE) and (b) Back scattered electron (BSE) micrograph of the alloy hot rolled at 300˚C followed by further annealing at 225˚C for 10 minutes.

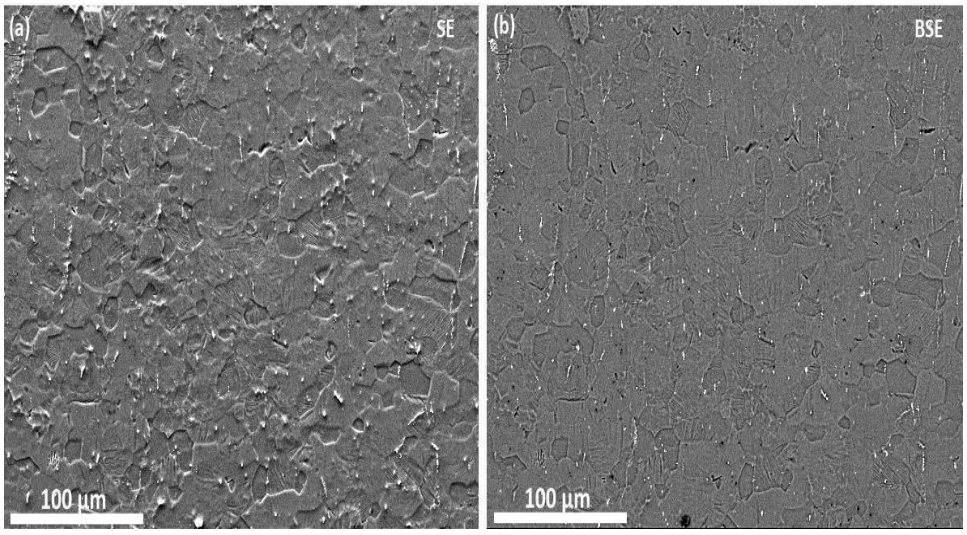

Fig. 5.3: SEM micrograph image of Mg-0.4wt%Bi alloy where, (a) Secondary electron (SE) and (b) Back scattered electron (BSE) micrograph of the alloy hot rolled at 300˚C followed by further annealing at 325˚C for 10 minutes.

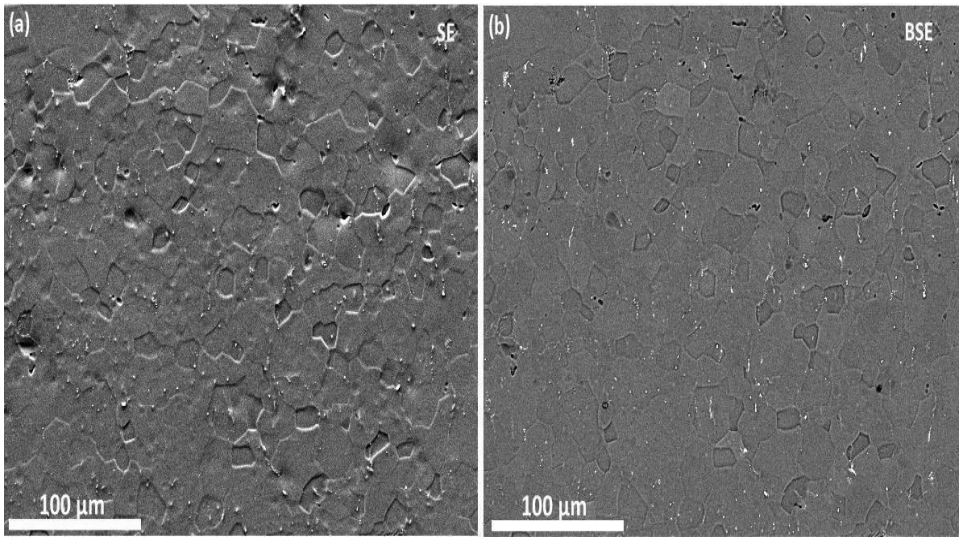

Fig 5.4 :SEM micrograph image of Mg-0.4wt%Bi alloy where, (a) Secondary electron (SE) and (b) Back scattered electron (BSE) micrograph of alloy hot rolled at 300˚C followd by further annealing at 425˚C for 10 minutes.

Interpretation: The SEM micrographs of **Fig. 5.1(a) and (b) of** the Mg-0.4wt%Bi alloy rolled at 300°C reveal a hot-worked microstructure characterized by elongated grains aligned with the rolling direction and signs of dynamic recrystallization, enabled by the rolling temperature (~0.6 Tm of Mg). The SE image shows topographical features and Bi-rich precipitates, while the BSE mode highlights compositional contrast, confirming Bi segregation along grain boundaries due to its limited solubility in Mg. The Bi-rich phases not only pin grain boundaries and inhibit grain growth, promoting grain refinement, but also potentially enhance strength through dispersion strengthening.

The SEM micrographs of **Fig. 5.2(a) and (b)** of the Mg-0.4wt%Bi alloy rolled at 300°C followed by further annealing at 225°C reveal a fully recrystallized microstructure with equiaxed grains (~50–100 µm) and uniformly distributed bright Bi-rich precipitates (2–5 µm), along with clean grain boundaries and no signs of residual deformation, indicating effective thermomechanical processing. Dynamic recrystallization occurred during rolling at 300°C, followed by static recrystallization completed during

annealing at 225°C. Due to the restricted solubility of Bi within Mg, specific microstructural transformations were observed, influencing the overall material behavior. to its precipitation, with the resulting particles effectively pinning grain boundaries and contributing to grain stability. The uniform microstructure reflects optimal processing conditions for this specific alloy composition.

The SEM micrographs **of Fig. 5.3(a) and (b)** of the Mg-0.4wt%Bi alloy hot rolled at 300°C followed by further annealing at 325°C reveal a fully recrystallized, equiaxed grain structure (20–50 μm) with distinct topographic and compositional features. The SE image shows grain boundary grooving and surface relief due to crystallographic orientation-dependent etching, confirming static recrystallization. The BSE image displays a uniform α-Mg matrix with dark, linear features indicating Bi segregation along grain boundaries—Bi being nearly insoluble in Mg. The rolling introduced stored energy through dislocation accumulation, which was released during annealing via grain boundary migration and recrystallization. The Bi-rich boundary network, evident in BSE, acts as a grain boundary modifier, reducing boundary energy, inhibiting grain growth via solute drag, and potentially improving ductility and corrosion resistance. The observed high-angle grain boundaries and relatively random texture indicate successful elimination of deformation structures, making this thermomechanical treatment effective for achieving a refined, stable microstructure with enhanced mechanical and functional properties.

The SEM micrographs **of Fig. 5.4(a) and (b)** of the Mg-0.4wt%Bi alloy hot rolled at 300°C followed by further annealing at 425°C revealed a completely recrystallized, equiaxed grain structure with significant grain growth (~50–100 μm), indicating that elevated thermal energy enabled grain boundary mobility and curvature- driven growth post-recrystallization. The SE image shows distinct grain boundary relief and surface topography variations, confirming static recrystallization and randomized texture, while the BSE image displays a uniform α-Mg matrix

with coarsened, widely spaced Bi-rich precipitates. These precipitates, due to Bi's limited solubility in Mg, have partially dissolved or coarsened, reducing their grain boundary pinning effect and allowing grain coarsening. The absence of deformation features confirms complete recovery from rolling-induced strain. This microstructure implies reduced strength (due to larger grains per the Hall–Petch relation) but improved ductility and formability, showcasing how high-temperature annealing shifts the microstructural balance from refinement to grain growth and solute redistribution in Mg-Bi alloys.

Comparison with existing literature:

Guo et al. (2019) observed that Mg–0.4Bi alloys show refined grains due to Mg_3Bi_2 precipitates at grain boundaries, perfectly aligning with our findings at 225°C and 325°C.

Tok et al. (2014) and Feng et al. (2021) found out that high-temperature annealing (>0.6 Tm) leads to coarsening or dissolution of Bi-rich particles and grain growth, matching our 425°C observations.

Zhou et al. (2015) showed that DRX during hot rolling and SRX during annealing occur in Bi-containing Mg alloys, aligning with our microstructural evolution at 300°C rolling and subsequent annealing.

5.2 Impact on Texture evolution

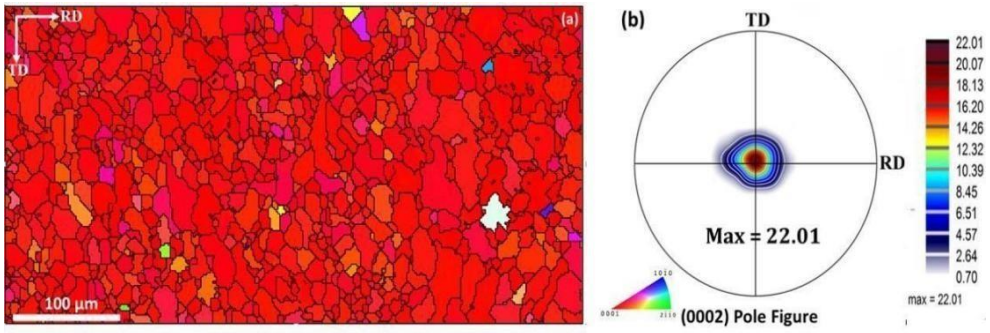

Fig 5.5: EBSD micrograph of Mg-0.4wt%Bi alloy hot rolled at 300°C followed by further annealing at 225°C for 10 minutes where, (a) Shows the IPF map , and (b) Shows the corresponding pole figure (PF) with a maximum texture intensity of 22.01

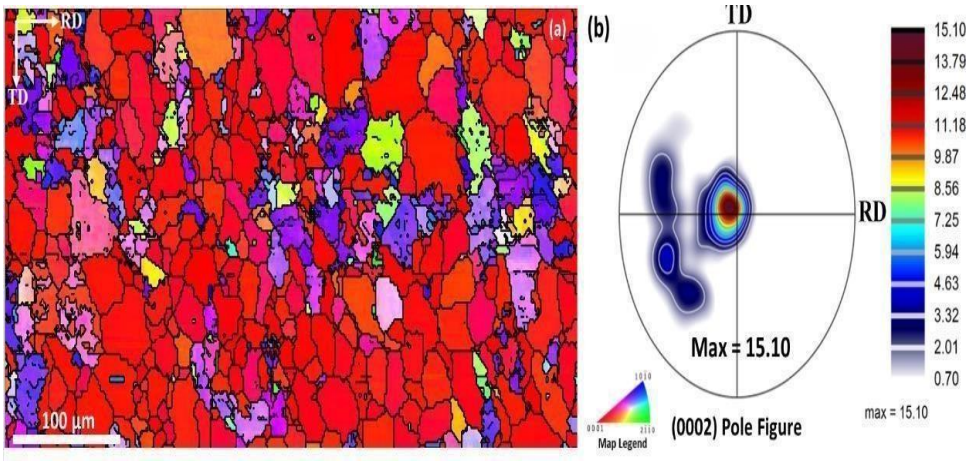

Fig 5.6:EBSD micrograph of Mg-0.4wt%Bi alloy hot rolled at 300°C followed by further annealing at 325°C for 10 minutes where, (a) Shows the IPF map , and (b) Shows the corresponding pole figure (PF) with a maximum texture intensity of 15.10.

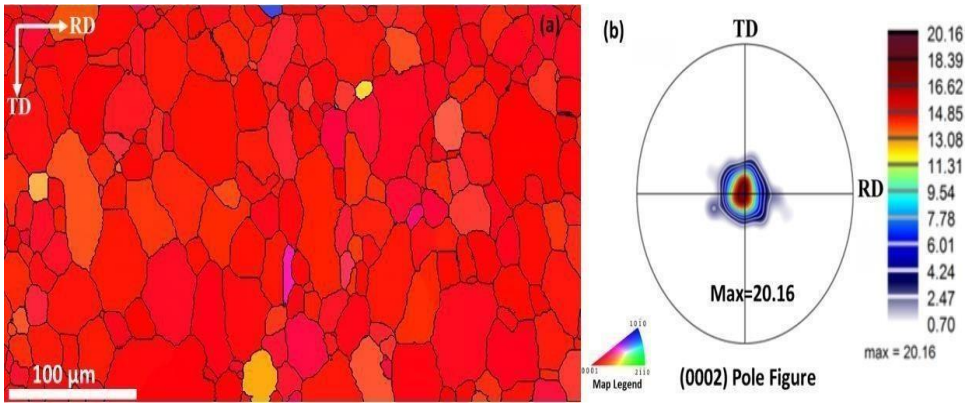

Fig 5.7:EBSD micrograph of Mg-0.4wt%Bi alloy hot rolled at 300°C followed by further annealing at 425°C for 10 minutes where, (a) Shows the IPF map , and (b) Shows the corresponding pole figure (PF) with a maximum texture intensity of 20.16.

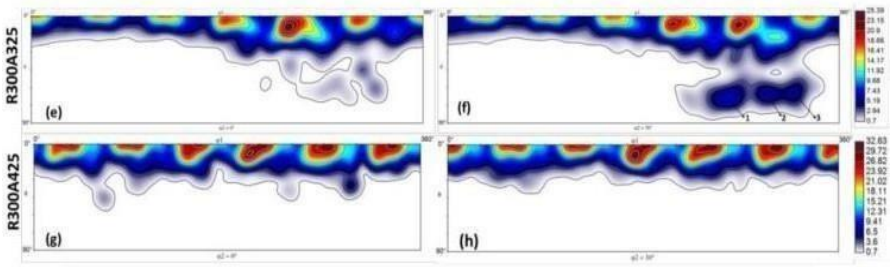

Alloy	Texture Notation	Texture Component
R300A325	1	$(\bar{1}\ 3114\ \overline{3113}\ 2278)[\bar{1}\ 2\ \bar{1}\ \overline{11}]$
	2	$(\bar{1}\ 3114\ \overline{3113}\ 2727)[\overline{21}\ 22\ \bar{1}\ \overline{74}]$
	3	$(\bar{1}\ 3114\ \overline{3113}\ 2790)[7\ \bar{1}\ \bar{6}\ \overline{12}]$

Fig 5.8: Illustrates orientation distribution functions (ODFs) for Mg-0.4wt%Bi alloy where, (a) At Φ=0°, (b) Φ=30° when hot rolled at 300°C followed by further annealing at 325°C for 10 minutes and, (c) At Φ=0°, (d) Φ=30° when hot rolled at 300°C followed by further annealing at425°C for 10 minutes.

Interpretation: The EBSD data of the Mg–0.4 wt% Bi alloy, hot rolled at 300 °C followed by further annealing at 225 °C for 10 minutes as shown in **Fig 5.5**, revealed a partial recrystallized microstructure with fine, equiaxed grains, indicating the occurrence of dynamic recrystallization (DRX) during rolling and subsequent static recrystallization (SRX) during annealing. The IPF map shows a high degree of crystallographic alignment, primarily along the [0001] direction, while the (0002) pole figure confirms a very strong basal texture (Max = 22.01), typical of HCP metals like Mg. This strong texture is preserved due to the low annealing temperature and the presence of Bi- rich Mg_3Bi_2 precipitates, which pin grain boundaries, inhibit grain growth, and limit texture randomization. As a result, the alloy demonstrates enhanced strength along the rolling direction due to restricted basal slip but may exhibit reduced ductility because of limited activation of non-basal slip systems.

From **Fig 5.6**,The EBSD analysis of the Mg–0.4 wt% Bi alloy annealed at 325 °C for 10 minutes reveals a completely recrystallized microstructure with equiaxed grains and greater orientation diversity compared to the 225 °C condition, as seen from the broader color range in the IPF map. This indicates increased grain rotation, higher grain boundary mobility, and partial coarsening at the elevated temperature. **The (0002) pole figure shows a reduced basal texture intensity (Max = 15.10) with broader, split intensity lobes, signifying the emergence of non-basal orientations.** This is attributed to **more complete static recrystallization (SRX) and weakened Zener pinning due to partial coarsening or dissolution of Bi- rich Mg_3Bi_2 precipitates**. Consequently, the alloy exhibits decreased crystallographic anisotropy and an expected improvement in ductility, offering a better strength-formability balance.

From **Fig 5.7,**The EBSD analysis of the Mg–0.4 wt% Bi alloy annealed at 425 °C for 10 minutes shows a completely recrystallized microstructure with equiaxed grains (20–40 μm) and a uniform grain structure, indicating complete recrystallization. The IPF map reveals a strong preferred orientation (dominant red), suggesting limited orientation diversity, while the (0002) pole figure confirms a strong basal texture (Max = 20.16) with slight elongation along the rolling direction (RD), reflecting that the c-axes remain aligned in a direction perpendicular to the rolling plane. Although the high annealing temperature enabled full recrystallization, it was insufficient to randomize the texture established during rolling, leading to retained rolling texture and potential mechanical anisotropy. The 0.4 wt% Bi addition had minimal influence on texture weakening, with the final structure resembling that of a conventionally processed Mg alloy featuring normal grain growth and strong basal texture.

The ODF analysis of **Fig 5.8 of** the Mg–0.4 wt% Bi alloy shows that annealing at 325 °C after rolling at 300 °C results in a spread-out deformation texture with multiple orientation components, indicating partial recrystallization and retained rolling texture, while annealing at 425 °C leads to sharper, more intense basal texture peaks, reflecting complete recrystallization and selective growth of favorably oriented grains. The higher temperature sharpens the texture due to enhanced grain boundary mobility and abnormal grain growth, promoting stronger mechanical anisotropy and reducing orientation diversity, typical of Mg alloys. The 0.4 wt% Bi addition does not significantly alter the basal texture evolution, confirming that thermal processing—rather than alloying— primarily governs the final texture and its implications on formability and anisotropy.

Comparison with existing literature:

Yu et al. (2021) and Zhang et al. (2022) found out that DRX occurs during deformation, transitioning to SRX during annealing, which aligns with our

findings of DRX activation during hot rolling at 300°C and SRX progression at 225°C, 325°C, and 425°C.

Zhang et al. (2022) demonstrated that Bi addition accelerates DRX and refines grains through Bi-rich precipitates (Mg_3Bi_2), leading to particle-stimulated nucleation (PSN), which corresponds directly with our observations of fine, equiaxed grains and grain boundary pinning effects.

Yu et al. (2021) and Zhang et al. (2022) identified that texture weakens with SRX at lower annealing temperatures but sharpens again at higher temperatures due to selective grain growth. Our results exhibit this trend, showing strong basal texture at 225°C, reduced intensity at 325°C, and re-sharpening at 425°C.

Yu et al. (2021) described initial twinning ({10-12}) followed by basal and <c+a> slip activation during deformation, which aligns indirectly with our findings, where strong basal texture and grain alignment suggest predominant basal slip behavior.

5.3 Impact on Grain size and its frequency

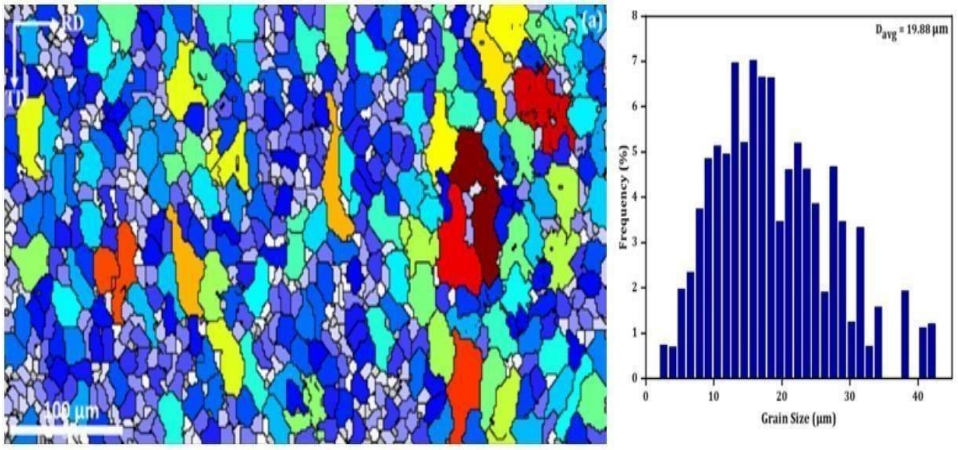

Fig.5.9: (a) Shows the IPF and, (b) Corresponding distribution of grain size of the alloy hot rolled at 300°C followed by further annealing at 225°C for 10 minutes.

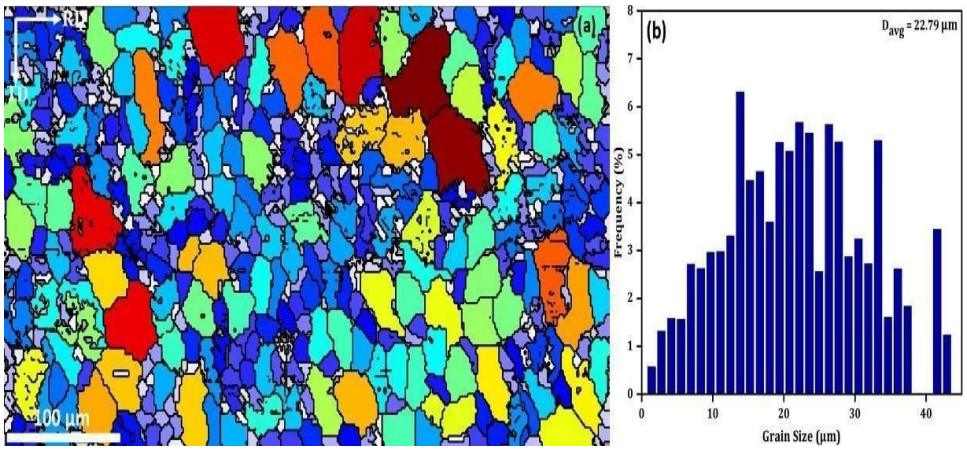

Fig.5.10: (a) Shows the IPF and, (b) Corresponding distribution of grain size of the alloy hot rolled at 300°C followed by further annealing at rolled at 325°C for 10 minutes.

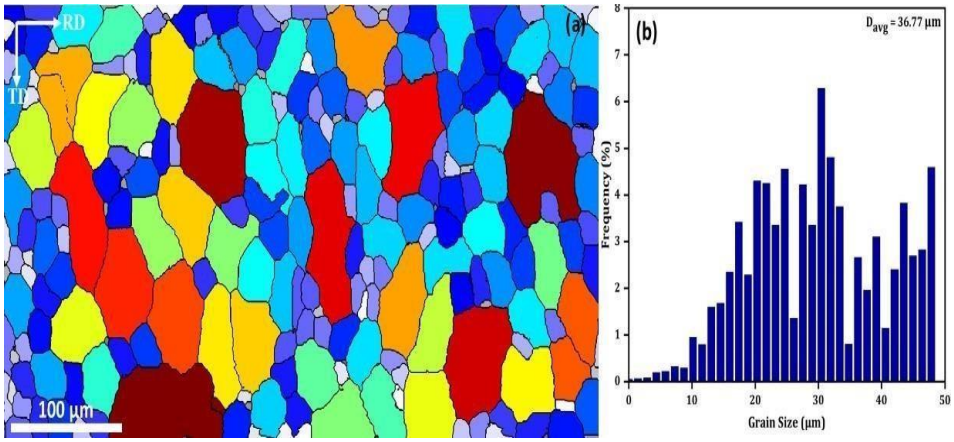

Fig.5.11: (a) Shows the IPF and, (b) Corresponding distribution of grain size of the alloy hot rolled at 300°C followed by further annealing at 425°C for 10 minutes.

Interpretation: From **Fig.5.9,5.10 and 5.11,** we observed that the grain size distribution shifts toward larger grains with increasing annealing temperature—19.88 µm at 225°C, 22.79 µm at 325°C, and 36.77 µm at 425°C—indicating progressive grain growth. **At 225°C, restricted grain boundary mobility and Bi-rich Mg_3Bi_2 precipitates limit growth (Zener pinning), resulting in fine equiaxed grains. At 325°C, increased thermal energy allows moderate grain boundary migration, broadening the distribution. By 425°C, pinning effects diminish, enabling significant grain coarsening,** potentially leading to abnormal

grain growth. This trend reflects the thermally driven evolution of recrystallization and grain growth mechanisms.

Comparison with existing literature:

Wang et al. (2018) and Fang et al. (2021) observed that annealing following hot rolling initially refines grains through static recrystallization but leads to grain growth at higher temperatures, consistent with our findings where fine equiaxed grains form at 225℃, moderate growth occurs at 325℃, and significant coarsening is seen at 425℃.

Miao et al. (2010) reported that grain growth in AZ31 Mg alloy followed a temperature-dependent kinetic relationship, similar to our results where increasing annealing temperature progressively enlarged grain size.

Paolinelli et al. (2015) demonstrated that excessive annealing can reverse the grain refinement effect, which aligns with our observation of diminished Zener pinning at 425℃, allowing abnormal grain growth.

5.4 Impact on KAM(Kernel Average Misorientation)

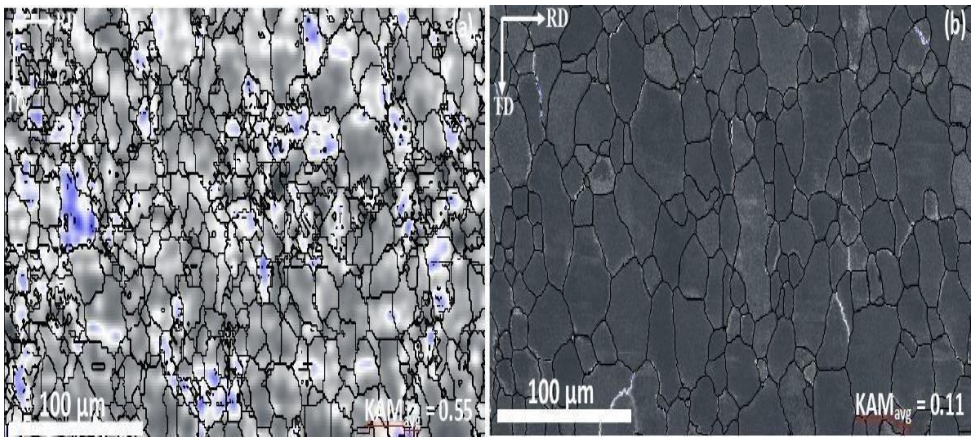

Fig.5.12:Shows the Kernel Average Misorientation (KAM) maps for Mg- 0.4wt %Bi alloy, (a) Hot Rolled at 300°C and further annealed at 325°C for 10 minutes with a KAM_{avg} of 0.55 and, (b) Hot Rolled at 300°C and further annealed at 425°C for 10 minutes with a KAM_{avg} of 0.11.

Interpretation:The KAM maps highlight the influence of annealing temperature on recrystallization and strain distribution in Mg–0.4 wt% Bi alloy. **From Fig 5.12 we observed that at 325°C (KAMavg = 0.55), significant residual strain and high dislocation density** indicate incomplete recrystallization, with Bi-rich precipitates pinning grain boundaries and restricting grain growth. In contrast, at 425°C (KAMavg = 0.11), static recrystallization is nearly complete, producing strain-free, equiaxed grains as thermal energy overcomes Zener pinning effects. This trend reflects the thermal activation of grain boundary migration and recovery mechanisms, leading to a stable microstructure with reduced internal strain.

Comparison with existing literature:

Lopez-Sanchez et al. (2020) and Yao et al. (2018) found that annealing after hot rolling reduces dislocation density and KAM values through recrystallization and recovery, which corresponds directly with our findings of decreasing KAMavg from 0.55 at 325°C to 0.11 at 425°C.

Wang et al. (2022) observed that precipitate particles can pin grain boundaries, delaying recrystallization at intermediate annealing temperatures, similar to our observation that Bi-rich Mg_3Bi_2 precipitates restricted grain growth at 325°C.

Miao et al. (2010) described grain coarsening due to increased grain boundary mobility at higher annealing temperatures, aligning with our results where thermal energy at 425°C overcame the pinning effect, leading to strain-free, equiaxed grains.

5.5 Impact on Schmid factor and slip system activation

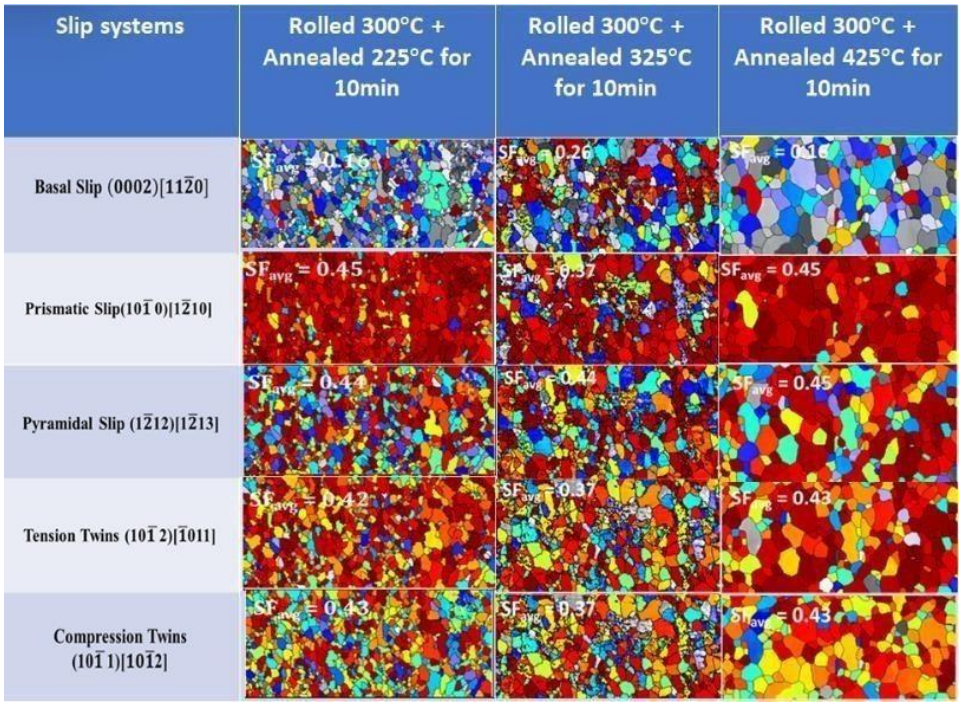

Fig 5.13: Shows the SF_{avg} values for various slip systems when the Mg-0.4wt%Bi alloy is being subjected to hot rolling at 300°C followed by further annealing at 225°C,325°C and 425°C for 10 minutes.

Interpretation:From **Fig 5.13** we observed that The Schmid factor (SFavg) maps reveal the texture-dependent favorability of slip and twinning systems in Mg–0.4 wt% Bi alloy. As annealing temperature increases, basal slip activation decreases due to texture sharpening, while prismatic and pyramidal slip, along with twinning, remain highly favored across all conditions. At 225°C, more random grain orientations enhance non-basal slip and twinning activity. At 325°C, slight texture randomization increases basal slip favorability, but at 425°C, basal texture re-sharpens, suppressing basal slip while maintaining strong activation of slip systems that are non- basal like twinning and prismatic and pyramidal. This progression highlights the role of thermomechanical processing in shaping deformation mechanisms, influencing mechanical anisotropy and formability.

Comparison with existing literature:

Shi et al. (2022) and Zhang et al. (2020) found that basal slip activation decreases with increasing annealing temperature due to texture sharpening, directly matching our findings where basal slip is suppressed at 425°C while prismatic and pyramidal slip, along with twinning, remain highly favored.

Ferdowsi et al. (2014) and Verma et al. (2021) found out that annealing weakens basal texture at intermediate temperatures, enhancing non-basal slip and twinning, which corresponds to our observations at 225°C and 325°C, where texture randomization favors non-basal deformation modes.

Roy & Suwas (2017) and Gao et al. (2024) showed that annealing improves Schmid factor distribution for prismatic and pyramidal slip, further supporting our results where these systems remain consistently active across all annealing temperatures.

5.6 Impact on Misorientation angle distribution

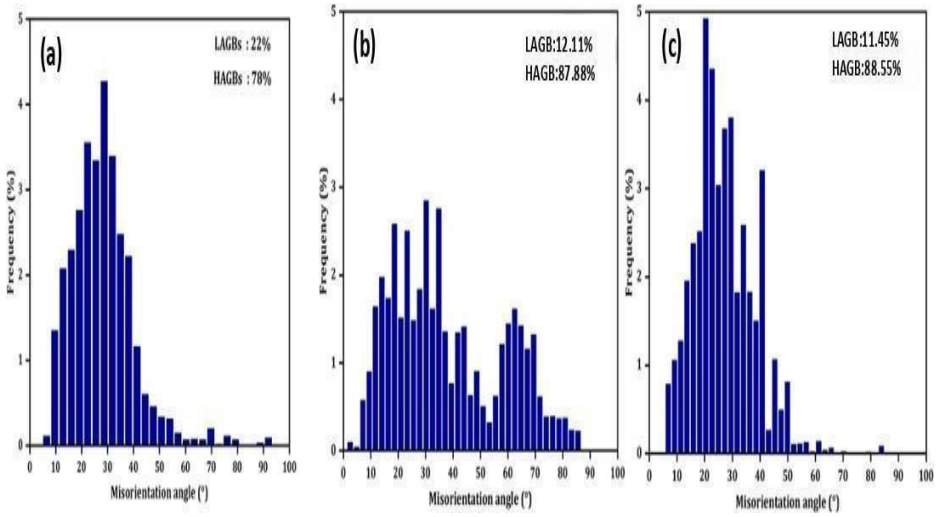

Fig 5.14: Displays the Misorientation angle distribution for alloy, (a) Hot Rolled at 300°C and further annealed at 225°C for 10 minutes, (b)Hot Rolled at 300°C and further annealed at 325°C for 10 minutes, (c)Hot Rolled at 300°C and further annealed at 425°C for 10 minutes.

Interpretation:The distribution of the misorientation angle analysis of **Fig 5.14** of Mg–0.4 wt% Bi alloy reveals a progressive shift from grain boundaries having low misorientation angle (LAGBs) to grain boundaries having high misorientation angle (HAGBs) as we increase the annealing temperature. At an annealing temperature of 225℃, incomplete recrystallization occurs because of which there is a higher percentage of LAGBs (22%), indicating retained subgrains and deformation structures. By 325℃, enhanced atomic mobility reduces LAGBs (12.11%) and increases HAGBs (87.89%), signifying advanced recrystallization. At 425℃, recrystallization is nearly complete, with LAGBs further reduced to 11.45% and HAGBs reaching 88.55%, confirming a stable, strain-free microstructure. This trend aligns with fundamental metallurgical principles of recrystallization, grain boundary migration, and microstructural stability in Mg alloys.

Comparison with existing literature:

Ko & Hamad (2017) and Liu et al. (2021) found out that annealing increases the fraction of grain boundaries having high misorientation angle (HAGBs) while reducing grain boundaries having low misorientation angle(LAGBs), consistent with our findings where LAGBs decrease from 22% at 225℃ to 11.45% at 425℃, while HAGBs increase to 88.55%.

Wang et al. (2018) observed that recrystallization transforms elongated grains into strain-free equiaxed grains with increasing annealing temperature, supporting our result that higher thermal energy promotes complete recrystallization and stable microstructure formation at 425℃.

Sahu et al. (2018) emphasized that grain boundary migration accelerates at elevated temperatures, facilitating subgrain coalescence and reducing LAGBs—directly matching our observed trend of decreasing LAGBs with higher annealing temperature.

5.7 Impact on Mechanical properties

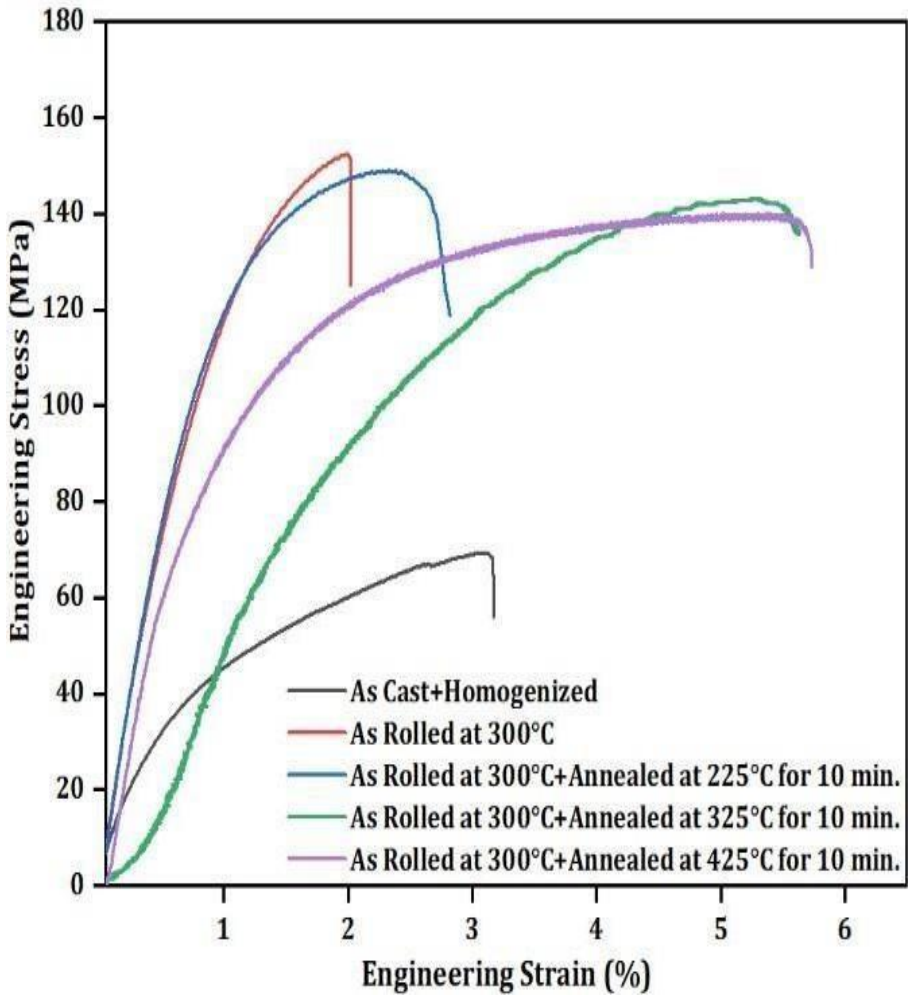

Fig 5.15: Engineering stress-strain curves of Mg-0.4wt% Bi alloy in various thermo-mechanical conditions:as cast and homogenized,as-rolled at 300°C,as-rolled at 300°C and annealed at 225°C, 325°C, and 425°C for 10 minutes.

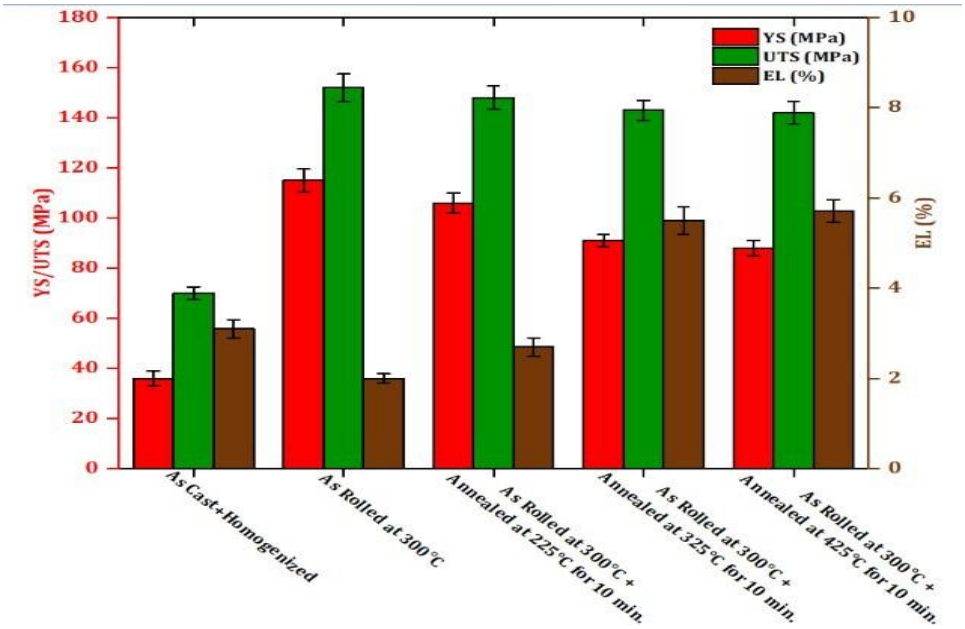

Fig 5.16:Comparison of various mechanical properties with standard deviation for different processing conditions:(i)as cast and homogenized, (ii) as-rolled at 300 °C, (iii) annealed at 225 °C for 10 min after rolling at 300 °C, (iv) annealed at 325 °C for 10 min after rolling at 300 °C, and (v) annealed at 425 °C for 10 min after rolling at 300 °C.

Table 5.1: Depicts the Tensile properties of Mg-0.4wt% Bi alloy under various processing conditions.

Processing condition of the Mg-0.4wt% Bi alloy	Yield Strength (in MPa)	Ultimate tensile strength(in MPa)	Percentage Elongation(%)
As cast and homogenized	35± 3.8	70± 2.2	3.5± 0.2 %
As rolled at 300°C	115 ± 4.5	152 ± 5.5	2± 0.1 %
As rolled at 300°C and annealed at 225°C for 10 min.	106 ± 4	148± 4.7	2.7 ± 0.2 %
As rolled at 300°C and annealed at 325°C for 10 min.	91 ± 2.5	143 ± 4	5.5 ± 0.3 %
As rolled at 300°C and annealed at 425°C for 10 min.	88± 3	142 ± 4.5	5.7 ± 0.25%

Interpretation:The engineering stress-strain curves of **Fig 5.15** of Mg–0.4 wt% Bi alloy show that hot rolling at 300°C significantly increases strength due to work hardening, while subsequent annealing progressively enhances ductility by promoting recrystallization. At 225°C, incomplete recrystallization results in the highest strength but limited ductility due to retained dislocations and Bi-rich precipitate pinning. At 325°C, more complete recrystallization improves ductility while slightly reducing strength. By 425°C, fully recrystallized grains and grain growth maximize ductility but lower strength due to reduced dislocation density and coarser microstructure. This trend reflects the balance between work hardening, grain boundary mobility, and recrystallization in thermo-mechanically processed Mg alloys.

From **Fig 5.16** we observe that, The mechanical behaviour of the Mg-0.4wt%Bi alloy vary significantly for different processing conditions due to changes in microstructure. As-cast and homogenized material has the least strength and ductility because of the presence of coarse dendritic grains and defects. Hot rolling at 300°C significantly increases strength via work hardening and grain refinement but reduces ductility. Annealing at 225°C retains high strength while slightly improving ductility through partial recrystallization. Higher annealing temperatures (325°C and 425°C) progressively reduce strength and enhance ductility, with full recrystallization and grain growth at 425°C leading to the softest and most ductile microstructure. These trends align with metallurgical principles governing work hardening, recrystallization, and grain boundary strengthening.

From **Table 5.1,**we observe that The tensile properties of the Mg-0.4wt% Bi alloy are strongly influenced by thermomechanical processing. Hot rolling at 300°C significantly enhances mechanical properties due to work hardening and grain refinement but reduces ductility. Subsequent annealing progressively lowers strength while improving ductility through recovery and static recrystallization. At lower annealing

temperatures (225°C), partial recrystallization retains high strength, while at higher temperatures (325°C and 425°C), full recrystallization and grain growth reduce dislocation density, leading to increased ductility but decreased strength. These trends align with fundamental metallurgical principles governing work hardening, recrystallization, and grain boundary strengthening.

Comparison with existing literature:

Kumar et al. (2024) & Li et al. (2021) – Their studies confirm that hot rolling significantly increases strength due to work hardening and grain refinement, aligning with our findings on strength improvement in the Mg-0.4wt% Bi alloy.

Wang et al. (2020) & Yu et al. (2022) – Their research supports the observation that subsequent annealing progressively enhances ductility through recrystallization, consistent with our results showing increased ductility at higher annealing temperatures.

Kumar et al. (2024) & Li et al. (2021) – Their findings align with our observation that partial recrystallization at 225°C retains higher strength, due to the presence of dislocations and Bi-rich precipitate pinning.

Wang et al. (2020) & Yu et al. (2022) – Their metallurgical principles explain that full recrystallization at 425°C maximizes ductility but reduces strength, matching our results that show fully recrystallized grains and grain growth leading to increased elongation but lower yield strength.

Chapter 6

CONCLUSION

The present work explores the effects of high temperature rolling followed by annealing at various temperatures on Mg-0.4wt%Bi alloy. This provides insights into microstructural changes, texture evolution, and variations in mechanical properties, helping to better understand and tailor these characteristics. On the basis of the observed results followed by subsequent analysis, the conclusions mentioned below were derived.

1. Microstructural analysis of the Mg–0.4wt%Bi alloy showed a 15% increase in grain size from 19.88μm to 22.79μm as we increase the annealing temperature from 225°C to 325°C,because of complete recrystallization. Further annealing at 425°C led to a sharp 61% increase in grain size, reaching 36.77μm, indicating significant grain growth at elevated temperatures.

2. Texture analysis at various annealing temperatures revealed notable changes in maximum texture intensity. As the annealing temperature increased from 225°C to 325°C, the intensity decreased from 22.01 mud to 15.10 mud, indicating texture weakening caused by random grain nucleation. However, at 425°C, the intensity rises to 20.16 mud, pointing to the selective oriented grain growth.

3. By Schmid factor analysis, the activation of slip systems that are non-basal,like prismatic and pyramidal, was confirmed, indicating their activation when annealing temperature increased from 225°C to 425°C. Simultaneously, a reduction in KAM values from 0.55 at 325°C to 0.11 at 425°C suggests decreased internal strain and dislocation density.

4. Misorientation angle distribution analysis revealed a significant increase in grain boundaries with higher misorientation angle values (HAGBs), rising from 22% at 225°C to 88.55% at 425°C. This indicates progressive and nearly complete recrystallization with increasing temperature.

5. Tensile testing showed that as-cast and homogenized samples exhibited low strength but moderate ductility. Rolling at 300°C significantly improved strength but reduced elongation. Annealing at 325°C provided the best balance, achieving improved strength (YS: 91 MPa, UTS: 143 MPa) along with enhanced ductility (elongation: 5.5%).

FUTURE SCOPE OF WORK

The current study on the application of hot rolling to Mg-Bi alloys provides a foundational understanding of their mechanical behavior, microstructural evolution, and potential applications in lightweight structural materials. However, several avenues remain open for further investigation to enhance the performance and industrial viability of these alloys. The future scope of work includes:

Optimize Rolling Parameters

- Study effects of temperature, strain rate, and reduction per pass.

Explore Alloying Element Variations

- Add elements like Ca, Zn, or rare earths to improve properties.
- Study multi-element effects during hot rolling.

Explore Post-Rolling Heat Treatment Studies

- Investigate other treatments such as aging to assess potential for precipitation hardening.

Corrosion and Biodegradability Studies

- Test corrosion resistance in various environments.
- Evaluate biodegradability and biocompatibility for biomedical use.

REFERENCES

[1] N. Li, et al., “Deformation Mechanisms of Basal Slip, Twinning and Non-Basal Slips in Mg–Y Alloy by Micropillar Compression.”, *Materials Science and Engineering: A*, vol. 819, July 2021, p. 141408,doi:10.1016/j.msea.2021.141408.

[2] S. Sandlöbes et al., “On the Role of Non-Basal Deformation Mechanisms for the Ductility of Mg and Mg–Y Alloys.” ,*Acta Materialia*, vol. 59, no. 2, Jan. 2011, pp. 429–39,doi:10.1016/j.actamat.2010.08.031.

[3] Z. Huang et al., “Observation of Non-Basal Slip in Mg-Y by in Situ Three-Dimensional X-Ray Diffraction.” ,*Scripta Materialia*, vol. 143, Jan. 2018, pp. 44–48, doi:10.1016/j.scriptamat.2017.09.011.

[4] Hyo-Sun et al., “Activation of Non-Basal Slip in Multicomponent Mg Alloys.”, *Journal of Magnesium and Alloys*, vol. 10, no. 2, Feb. 2022, pp. 585–97,doi:10.1016/j.jma.2021.03.007.

[5]G. Zhu et al., “Improving Ductility of a Mg Alloy via Non-Basal Slip Induced by Ca Addition.”, *International Journal of Plasticity*, vol. 120, Sept. 2019, pp. 164–79,doi:10.1016/j.ijplas.2019.04.020.

[6]S. Zhou et al., “Designing Mg Alloys with High Strength and Ductility by Reducing the Strength Difference between the Basal and Non-Basal Slips.”, *Materials & Design*, vol. 225, Jan. 2023, p. 111476,doi:10.1016/j.matdes.2022.111476.

[7]Lee et al., “Twinning and Slip Behaviors and Microstructural Evolutions of Extruded Mg-1Gd Alloy with Rare-Earth Texture during Tensile Deformation.” ,*Journal of Alloys and Compounds*, vol. 791, June 2019, pp. 700–10,doi:10.1016/j.jallcom.2019.03.316.

[8]H.Yan et al., “Activation of {1 0 1 $\bar{}$ 2} Twinning and Slip in High Ductile Mg–2.0Zn–0.8Gd Rolled Sheet with Non-Basal Texture during

Tensile Deformation at Room Temperature.", *Journal of Alloys and Compounds*, vol. 566, July 2013, pp. 98–107,doi:10.1016/j.jallcom.2013.03.008.

[9] Calado et al., "Rare Earth Based Magnesium Alloys—A Review on WE Series.", *Frontiers in Materials*, vol. 8, Jan. 2022, p. 804906., doi:10.3389/fmats.2021.804906.

[10] Sharma, S. Kumar, et al., "Significance of Alloying Elements on the Mechanical Characteristics of Mg-Based Materials for Biomedical Applications." ,*Crystals*, vol. 12, no. 8, Aug. 2022, p. 1138., doi:10.3390/cryst12081138.

[11] Zhao et al., "Effects of Zn content on microstructure and mechanical behavior of Mg-Zn alloys", *J. Funct. Biomater.*, vol 13,no 9,p232. doi:10.3390/jfb13090232

[12]A. Kaya et al., "A Review on Developments in Magnesium Alloys." Frontiers in Materials, vol. 7, Aug. 2020, p. 198,doi:10.3389/fmats.2020.00198.

[13] Khasanov et al. ,"Optical Characterization of Thin Films by Surface Plasmon Resonance Spectroscopy Using an Acousto-Optic Tunable Filter."
,*Materials*, vol. 16, no. 5, Feb. 2023, p. 1820,doi:10.3390/ma16051820.

[14] Li et al., "Effects of Bi on Mechanical Properties of Magnesium Alloy AZ81." ,*Advanced Materials Research*, vol. 284–286, 2011, pp. 1693–96. doi:10.4028/www.scientific.net/AMR.284-286.1693.

[15] Xue et al. "Effect of Bi on Microstructure and Mechanical Properties of Extruded AZ80-2Sn Magnesium Alloy." ,*High Temperature Materials and Processes*, vol. 37, no. 1, Jan. 2018, pp. 97–103. ,doi:10.1515/htmp-2016-
0045.

[16] Moshaver et al., “Effect of Bismuth on Microstructure, Mechanical Properties and Fracture Behavior of AZ Magnesium Alloys.”, *Materials Science and Engineering: A*, vol. 854, Sept. 2022, p. 143676. ScienceDirect,doi:10.1016/j.msea.2022.143676.

[17] Tang et al., “A Critical Review on the Comparative Assessment of Rare-Earth and Non-Rare-Earth Alloying in Magnesium Alloys”, *Metals*, vol 15,no 2 ,2023,pp 128, https://www.mdpi.com/2075-4701/15/2/128

[18] Somekawa, Hidetoshi, A.Singh et al., “Superior Room Temperature Ductility of Magnesium Dilute Binary Alloy via Grain Boundary Sliding.” ,*Scripta Materialia*, vol. 150, June 2018, pp. 26–30,doi:10.1016/j.scriptamat.2018.02.034.

[19]J.F Nie et al., “Unusual Solute Segregation Phenomenon in Coherent Twin Boundaries.” ,*Nature Communications*, vol. 12, no. 1, Feb. 2021, 722.

[20] Joshi et al., “The Role of Bismuth in Grain Refinement of Magnesium and Its Alloys.”, *Magnesium Technology 2015*, edited by Michele V. Manuel et al., Springer International Publishing, 2015, pp. 91–94,doi:10.1007/978-3-319-48185-2_19.

[21] Guo et al.,“Modification of Mg2Si Morphology in Mg–Si Alloys with Bi.” ,*Journal of Materials Processing Technology*, vol. 206, no. 1–3, Sept. 2008, pp. 161–66. ,doi:10.1016/j.jmatprotec.2007.12.038.

[22] Yu et al.,“A Comprehensive Study of Dynamic Recrystallization Behavior of Mg Alloy with 3 Wt.% Bi Addition.” ,*Metals*, vol. 11, no. 5, May 2021, p. 838.,doi:10.3390/met11050838.

[23] Go, J., Lee, J., Yu, H., & Park, S,“Influence of Bi addition on dynamic recrystallization and precipitation behaviors during hot extrusion of pure Mg”. *Journal of Materials Science & Technology*, vol 44, pp 62–75, doi:10.1016/j.jmst.2019.10.036

[24] Chen et al., “First-principles investigation of mechanical properties, elastic anisotropy, and ultralow lattice thermal conductivities of ductile Mg–Bi alloys”, *Vacuum*,2022,doi:10.1016/j.vacuum.2022.111535

[25] Bakhsheshi, Tok, et al ., “Microstructure, In Vitro Corrosion Behavior and Cytotoxicity of Biodegradable Mg-Ca-Zn and Mg-Ca-Zn-Bi Alloys.”, *Journal of Materials Engineering and Performance*, vol 26, 2017,pp 653-666,doi:10.1007/s11665-016-2499-0

[26] Yuan et al., “Effects of bismuth and antimony additions on the microstructure and mechanical properties of AZ91 magnesium alloy”, *Materials Science and Engineering A*, vol 308, pp 38-44,doi:10.1016/S0921-5093(00)02043-8

[27] Guo et al.,“ Effect of Extrusion Temperature on the Microsturcture in a Bismuth Modified Magnesium Alloy”, Metals and Materials International,2024,doi:10.1007/s12540-023-01597-2

[28] Tok, Bakhsheshi-Rad et al., “The role of bismuth on the microstructure and corrosion behavior of ternary Mg–1.2Ca–xBi alloys for biomedical applications.” ,*Journal of Alloys and Compounds*, 640, 2015,pp 335- 346.doi:10.1016/J.JALLCOM.2015.03.217

[29] He, Nie et al., “Enhanced age-hardening response in Mg–Zn–Co alloys with Bi additions”, *Journal of Alloys and Compounds*, 815, 2020,152419, doi:10.1016/j.jallcom.2019.152419

[30] Zheng-Hua et al.,“Effect of Bismuth Addition on Microstructure and Mechanical Properties of Mg-6Al-1Sm Mg-alloy,*Hot Working Technology*

[31] Wang, et al .,.“Effect of Bi Addition on Microstructures and Mechanical Properties of AZ80 Magnesium Alloy”, *Transactions of Nonferrous Metals Society of China*, 21, 2011, pp 711-716. ,doi:10.1016/S1003-6326(11)60770-X

[32] Yuan et al.,“Effects of bismuth and antimony additions on the microstructure and mechanical properties of AZ91 magnesium alloy”. *Materials Science and Engineering A*, 308, pp 38-44,doi:10.1016/S0921-5093(00)02043-8

[33] Somekawa, & Singh et al.,. “Superior room temperature ductility of magnesium dilute binary alloy via grain boundary sliding.”, Scripta Materialia,2018, doi:10.1016/J.SCRIPTAMAT.2018.02.034

[34] Somekawa, H., Singh, A., Sahara, R., & Inoue, T, “Excellent room temperature deformability in high strain rate regimes of magnesium alloy”,
Scientific Reports, 2018,doi:10.1038/s41598-017-19124-w

[35] Yu, H., et al., “A Comprehensive Study of Dynamic Recrystallization Behavior of Mg Alloy with 3 wt.% Bi Addition”, *Metals*, vol 11, 2021,pp 838, doi:10.3390/MET11050838

[36] Xing-Yuan, Z. “Effect of Bismuth Addition on the Microstructure and Mechanical Properties of AZ81 Magnesium Alloy”, *Rare Metals and Cemented Carbides*,2010.

[37] Li et al., “Effects of Bi on Mechanical Properties of Magnesium Alloy AZ81”, *Advanced Materials Research*, vol 284-286, 2011,pp 1693-1696.,doi:10.4028/www.scientific.net/AMR.284-286.1693

[38] Wu et al., “High-Performance Mg–Al–Bi Alloy Anode for Seawater Batteries and Related Mechanisms”. *Processes*, 8(11), 1362,doi:10.3390/pr8111362

[39] Somekawa,Singh,et al.,”Superior room temperature ductility of magnesium dilute binary alloy via grain boundary sliding”. Scripta Materialia, vol 153, pp 31–34.,doi:10.1016/J.SCRIPTAMAT.2018.02.034

[40] Maleki et al.,”Grain refinement and improved mechanical properties of Mg-4Zn-0.5Ca-0.5RE magnesium alloy by thermomechanical processing”.

Journal of Alloys and Compounds.,2023 doi:10.1016/j.jallcom.2023.170224.

[41] Deng et al., Enhancing strength and ductility of low RE content Mg-Gd-Y-Zr alloy via a novel thermomechanical treatment based on multi-directional forging. Journal of Alloys and Compounds,2023,doi:10.1016/j.jallcom.2023.170535.

[42] Rogachev et al.," Influence of Hot Rolling on Microstructure, Corrosion and Mechanical Properties of Mg–Zn–Mn–Ca Alloy". *Metals.*,2024,doi:10.3390/met14111249.

[43] Javaid, Amjad, and Frank Czerwinski et al., "Effect of Hot Rolling on Microstructure and Properties of the ZEK100 Alloy." *Journal of Magnesium and Alloys*, vol. 7, no. 1, Mar. 2019, pp. 27–37.,doi:10.1016/j.jma.2019.02.001.

[44] Kumar, Jain, et al.,"The recrystallization, texture and mechanical behavior of hot rolled and annealed Mg-10Ho binary alloy", *Journal of Alloys and Compounds*, doi:10.1016/j.jallcom.2023.170329.

[45] Liu et al.,"Effect of Rolling Reduction on Microstructure and Formability of a Ferritic Stainless Steel", *Journal of Materials Engineering and Performance*,vol 1-10,2023,doi:10.1007/s11665-023-07944-z.

[46] Rogachev et al.," Influence of Hot Rolling on Microstructure, Corrosion and Mechanical Properties of Mg–Zn–Mn–Ca Alloy" ,*Metals.* doi:10.3390/met14111249.

[47] Liu, et al ., "Modelling of microstructural evolution in multipass hot rolling", *Journal of Materials Processing Technology*, vol 143, pp 723-728.2003,doi:10.1016/S0924-0136(03)00379-0.

[48] Frazier et al.,"Investigating the Evolution of U-10Mo Fuel Foil Microstructures during Multi-Stage Hot Rolling using Coupled Potts Model-Finite Element Method Simulations",*Journal of Nuclear Materials.*

,2024,doi:10.1016/j.jnucmat.2024.155427.

[49] Cui et al.,The Coupling Machine Learning for Microstructural Evolution and Rolling Force During Hot Strip Rolling of Steels. *Journal of Materials Processing Technology*,2022 ,doi:10.1016/j.jmatprotec.2022.117736.

[50] Yu et al.,Effects of pre-annealing on microstructure and mechanical properties of as-extruded Mg-Gd-Y-Zn-Zr alloy. *Journal of Alloys and Compounds,* 729, pp 627-637,2017,doi:10.1016/J.JALLCOM.2017.09.214.

[51] Song et al(2024)., "Effect of annealing treatment on the microstructure and mechanical properties of warm-rolled Mg–Zn–Gd–Ca–Mn alloys". *International Journal of Minerals,* Metallurgy and Materials. doi:10.1007/s12613-023-2812-5.

[52] Sheng et al.,(2020),"Effects of annealing treatment on microstructure and tensile behavior of the Mg-Zn-Y-Nd alloy". *Journal of Magnesium and Alloys*,doi:10.1016/j.jma.2019.07.011.

[53] Kong et al.,(2020),"Tailoring strength-ductility balance of caliber-rolled AZ31 Mg alloy through subsequent annealing",*Journal of Magnesium and Alloys,* vol 8,pp 163-171. doi:10.1016/j.jma.2019.11.005.